Linker Length Modulates DNA Cross-Linking Reactivity and Cytotoxic Potency of C8/C8′ Ether-Linked C2-*exo*-Unsaturated Pyrrolo[2,1-*c*][1,4]benzodiazepine (PBD) Dimers

Stephen J. Gregson,[†] Philip W. Howard,[†] Darren R. Gullick,[†] Anzu Hamaguchi,[‡] Kathryn E. Corcoran,[†] Natalie A. Brooks,[‡] John A. Hartley,[‡] Terence C. Jenkins,[§] Sejal Patel,[∥] Matthew J. Guille,[∥] and David E. Thurston*[,†]

Cancer Research UK Gene Targeted Drug Design Research Group, The School of Pharmacy, University of London, 29/39 Brunswick Square, London WC1N 1AX, U.K., Cancer Research UK Drug−DNA Interactions Research Group, Department of Oncology, University College London, 91 Riding House Street, London W1W 7BS, U.K., Yorkshire Cancer Research Laboratory of Drug Design, Tom Connors Cancer Research Centre, University of Bradford, All Saints Road, Bradford, West Yorkshire BD7 1DP, U.K., and Genes and Development, Institute of Biomedical and Biomolecular Sciences, University of Portsmouth, St Michael's Building, White Swan Road, Portsmouth, Hampshire PO1 2DT, U.K.

Received May 15, 2003

A C2/C2′-*exo*-unsaturated pyrrolo[2,1-*c*][1,4]benzodiazepine (PBD) dimer **4b** (DRG-16) with a C8−O$(CH_2)_n$O−C8′ diether linkage ($n = 5$) has been synthesized that shows markedly superior in vitro cytotoxic potency (e.g., >3400-fold in IGROV1 ovarian cells) and interstrand DNA cross-linking reactivity (>10-fold) compared to the shorter homologue **4a** (SJG-136; $n = 3$). In contrast, for the C-ring unsubstituted series, the corresponding $n = 5$ dimer (**3c**) is generally less cytotoxic and has a lower interstrand cross-linking reactivity compared to its shorter $n = 3$ homologue (**3a**). Dimer **4b** cross-links DNA with >10-fold efficiency compared to **4a**, and also inhibits the activity of the restriction endonuclease *Bam*H1 more efficiently than either **3a** or **4a**. The C2-*exo*-unsaturated PBD dimers **4a**,**b** are not only more effective than their C-ring saturated counterparts in terms of induced ΔT_m shift, but they also exert this effect more rapidly. Thus, while **3a** and **3c** exert 68 and 35% of their maximum effect immediately upon interaction with DNA, this level increases to 76 and 97% for **4a** and **4b**, respectively. Molecular modeling shows a rank order of **4b** ($n = 5$) > **4a** ($n = 3$) > **3a** ($n = 3$) > **3c** ($n = 5$) in terms of binding energy toward duplexes containing embedded target 5′-**G**AT_{1-2}C cross-link sequences, reflecting the superior fit of the C2-*exo*-unsaturated rather than saturated C-rings of the PBD dimers. A novel synthesis of core synthetic building blocks for PBD dimers via stepwise Mitsunobu reaction and nitration with $Cu(NO_3)_2$ is also reported.

Introduction

The pyrrolo[2,1-*c*][1,4]benzodiazepines (PBDs) such as DC-81 (**1**), tomaymycin (**2a**), and anthramycin (**2b**) are a family of tricyclic antitumor antibiotics that bind to minor groove DNA sites that span three base pairs (bp), preferably 5′-A**G**A, through a covalent bond to the exocyclic C2-NH_2 of the central guanine[1] (Figure 1). The first C8/C8′-linked PBD dimer (**3a**, DSB-120) was reported in 1992 in which two DC-81 (**1**) units were joined through their aromatic A-ring phenol positions by an inert propyldioxy linkage[2] (Figure 1). Homologous diether-linked dimers **3b**−**d** (i.e., −O−$(CH_2)_n$−O− where $n = 4-6$) were synthesized via a similar route,[3] and their relative in vitro cytotoxicities and interstrand DNA cross-linking efficiencies have been reported,[4] together with their cellular pharmacology.[5] Kamal and co-workers have also reported a series of PBD dimers of similar structure which lack one of the N10−C11/N10′−C11′ imine moieties and are thus incapable of cross-linking DNA.[6]

The $n = 3$ (**3a**) and longer $n = 5$ (**3c**) dimers show similar DNA cross-linking activity ($C_{50} = 0.055/0.070$ μM, respectively, toward plasmid pBR322), but are ≥10-fold more potent than the $n = 4$ (**3b**) and $n = 6$ (**3d**) homologues.[4,7] Dimers **3a** and **3c** showed similar in vitro cytotoxicity in two cell lines examined (K562 cells: $IC_{50} = 0.2/0.5$ μM; ADJ/PC6 cells: 0.0005/0.0004 μM, respectively), although **3c** is more potent in CH1 (0.00032 versus 0.003 μM) and leukemia L1210 cells (0.0045 versus 0.01 μM).[4] In agreement with their poor DNA reactivity, **3b** and **3d** showed much lower potency in all cell lines. Molecular modeling and NMR structural studies confirmed that **3a** spans 6 bp in the minor groove of duplex DNA, covalently binding to spatially separated guanines on opposite strands via their *exo*-cyclic C2−NH_2 groups and preferentially targeting 5′-Pu-***G****ATC*-Py tracts[7−10] (e.g., similar to **4a** shown in Figure 2A). The alternating pattern of behavior for $n =$ odd > $n =$ even dimers is interpreted in terms of minor groove accommodation of the ligands and conformational factors dictated by the inter-guanine separation for cross-linking.[7]

* Address correspondence to David E. Thurston, Professor of Anticancer Drug Design, The School of Pharmacy, University of London, 29/39 Brunswick Square, London WC1N 1AX, U.K. Phone: [044] (0)207-753-5932. E-Mail: david.thurston@ulsop.ac.uk; Fax: [044] (0)207-753-5935.

[†] University of London.
[‡] University College London.
[§] University of Bradford.
[∥] University of Portsmouth.

10.1021/jm030897l CCC: $27.50
Published on Web 01/30/2004

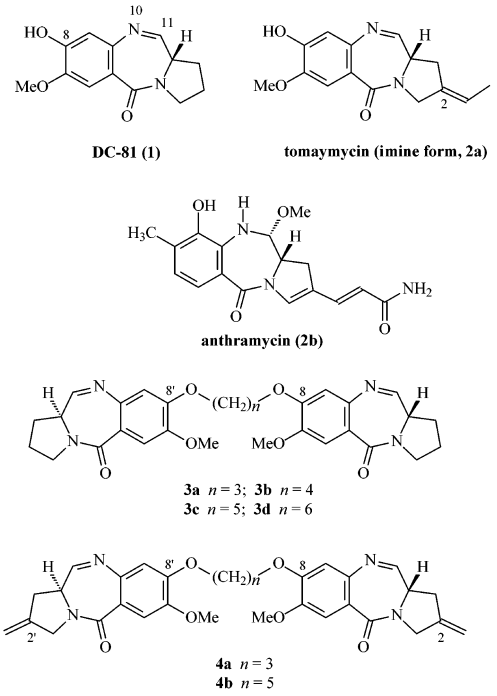

Figure 1. Structures of PBD monomers and dimers (see text).

However, **3a** lacks in vivo antitumor activity[11] despite marked in vitro cytotoxic potency.[2,4] This was attributed to excessive electrophilicity at the N10−C11 imine moieties, with the result that the molecule fails to reach the tumor in sufficient concentration due to collateral alkylation of proteins and other biological nucleophiles.[11,12] Dimer **4a** (SJG-136) containing C2/C2′-*exo*-methylene functionalities was subsequently designed to reduce the electrophilicity of the molecule.[13,14] This molecule shows significant in vivo potency and has been selected for clinical trials.[15,16]

We now report that lengthening the $-O(CH_2)_nO-$ linker of **4a** from $n = 3$ to 5 (i.e., **4a** → **4b**) effects an unexpected enhancement of DNA reactivity and in vitro cytotoxicity, in contrast to homologous extension of their C-ring unsubstituted counterparts (i.e., **3a** → **3c**). In addition to the greater length of DNA spanned upon binding compared to the shorter **4a** homologue (i.e., 7 bp for **4b/3c** rather than 6 bp for **4a/3a**) which confers greater adduct stability (i.e., **2B** vs **2A** in Figure 2), this behavior can be further explained by the superior isohelical fit of the C2-*exo*-methylene-substituted C-rings within the host DNA minor groove compared to the unsubstituted DC-81-type subunits (i.e., **4b** > **3c**).

Scheme 1[a]

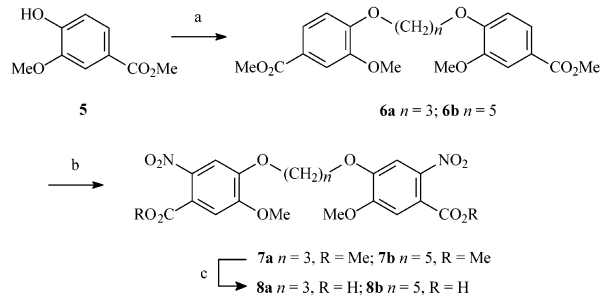

[a] (a) $HO(CH_2)_nOH/PPh_3$/DEAD/THF, 0 °C, 16 H, 58% (**6a**, $n = 3$), 52% (**6b**, $n = 5$); (b) $Cu(NO_3)_2/Ac_2O$, 1 h, 89% (**7a**), 98% (**7b**); (c) aq. NaOH/THF, 3 days, 100% (**8a**, **8b**).

Results and Discussion

Chemistry. Mitsunobu etherification of methyl vanillate **5** with either 1,3-propanediol or 1,5-pentanediol gave bis-esters **6a**−**b** in moderate yield (Scheme 1). This method was more convenient than the previously reported Williamson ether synthesis[13,14] due to facile extraction of the diether products and shorter reaction time. The nitro groups were introduced regioselectively using $Cu(NO_3)_2/Ac_2O$ to provide **7b** in high yield. Unlike alternative methods, this nitration reaction is not scale-limited. Quantitative ester hydrolysis afforded the key pentyl-linked dimer acid **8b**. This procedure was similarly used to generate the 1,3-propane core intermediate

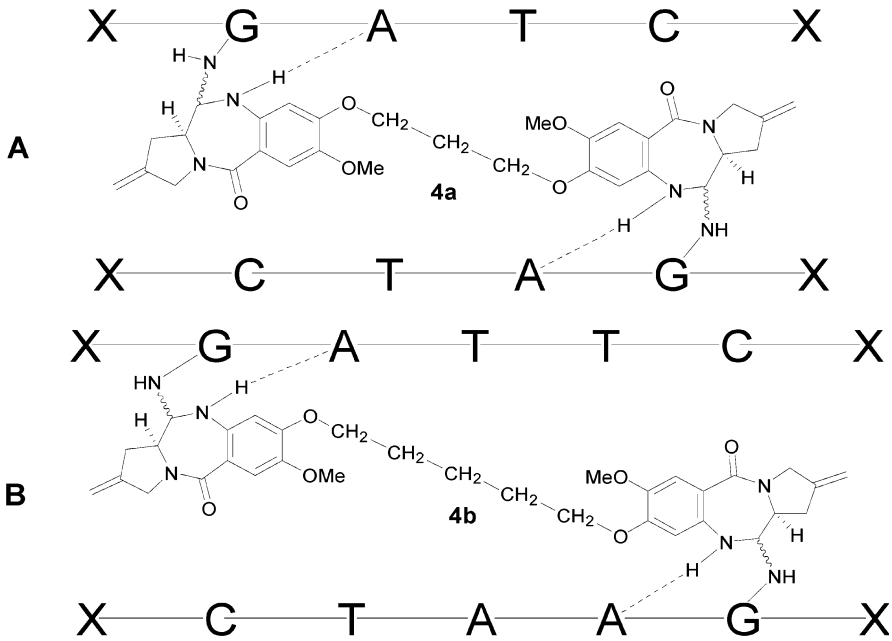

Figure 2. Schematic representation of the preferred DNA binding sites of dimers **4a** (A) and **4b** (B) which span six and seven DNA base pairs, respectively. Figure 2B shows an added spanned T-A base pair (X = purine or pyrimidine base).

Scheme 2[a]

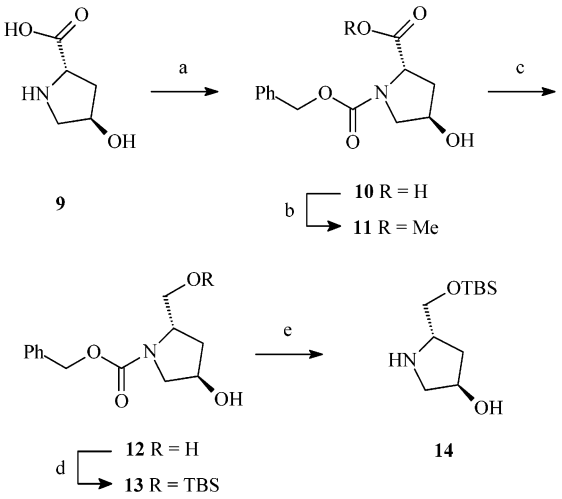

[a] (a) CBzCl, $PhCH_3$, $NaHCO_3$ (aq), 16 h, 99%; (b) MeOH, H_2SO_4, △, 3 h, quant; (c) $LiBH_4$, THF, 16 h, 96%; (d) TBS-Cl, TEA, DBU, CH_2Cl_2, 16 h, 78%; (e) 10% Pd-C, H_2, EtOH, 8 h, 99%.

(**8a**; $n = 3$) from ester **6a** in higher yield than previously reported.[13,14]

The key PBD C-ring coupling fragment **14** was prepared in five high-yielding steps from *trans*-4-hydroxy-L-proline **9** (Scheme 2). Following quantitative *N*-CBz protection[17] and esterification (**10** → **11**), the methyl ester **11** was reduced to diol **12** in 96% yield using $LiBH_4$ in THF. The primary alcohol was then selectively protected as a TBS ether (**13**) and the CBz protecting group cleaved by hydrogenolysis to provide the free amine **14**.

The 1,3-propane and 1,5-pentane diether-linked dimer cores **8a**−**b** were activated to the corresponding acid chlorides and coupled to the secondary amine **14** to provide the bis-amides **15a**−**b** in good yield (Scheme 3). Following high yielding reduction of the nitro groups, the resulting bis-anilines **16a**−**b** were treated with allyl chloroformate and pyridine to provide the bis-carbamates **17a**−**b**. Next, the secondary hydroxyl groups were oxidized under Swern conditions to bis-ketones **18a**−**b** in high yield. The key C2-*exo* unsaturation was introduced into the molecules using the Wittig reaction to give **19a** in 51% yield and **19b** in disappointing 35% yield. However, unreacted ketone could be recovered by chromatography and subjected to a further Wittig reaction to obtain more product. The TBS protecting groups were then cleaved (96−99% yield) and the resulting bis-alcohols **20a**−**b** oxidized to generate the PBD B-ring (**21a**−**b**). Yields from the Swern mediated cyclization were low (28%) for the 1,5-pentane diether linked compound **21b** and high (77%) for the 1,3-

Scheme 3[a]

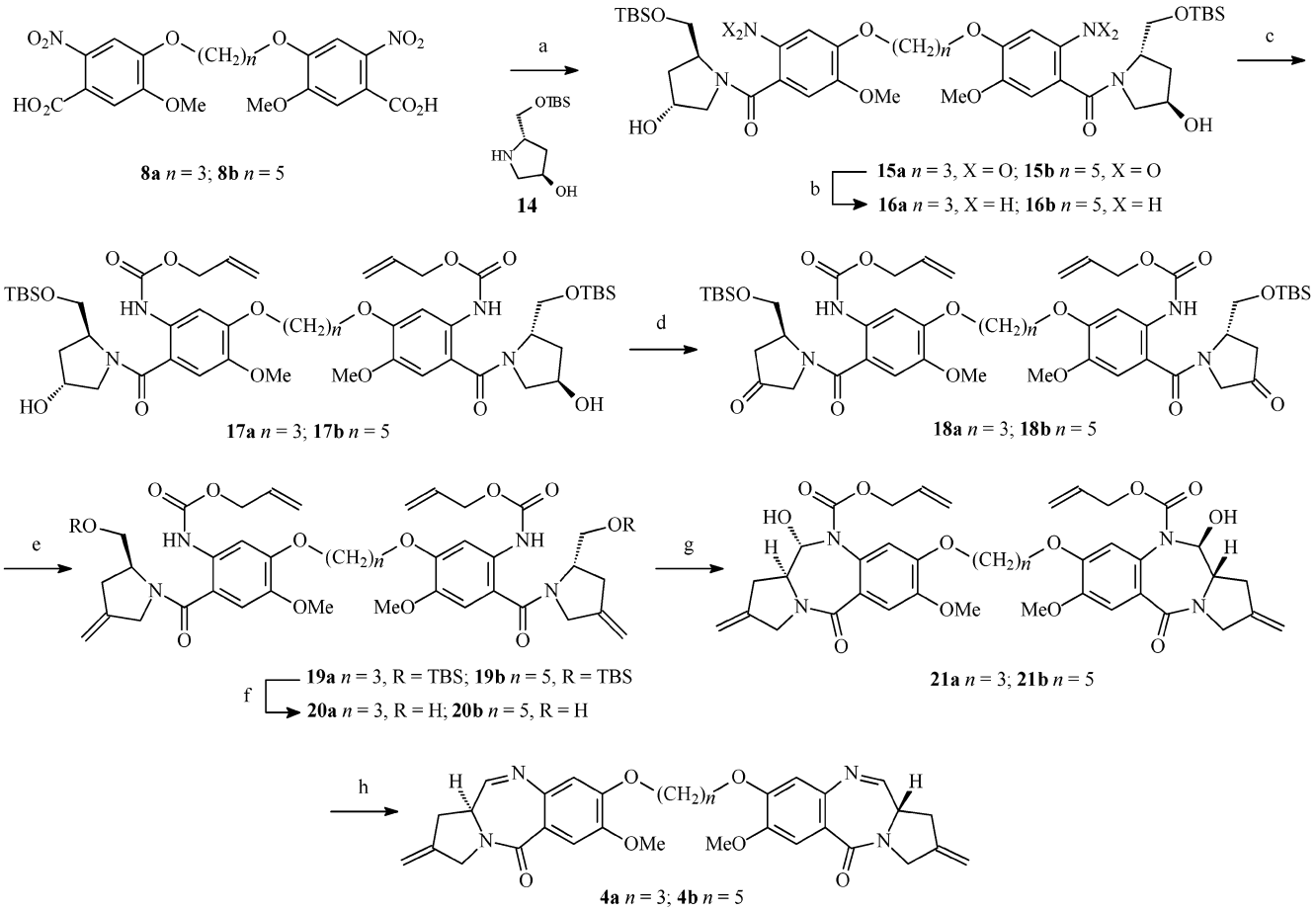

[a] (a) $(COCl)_2$/DMF/THF, 16 h, then **14**, TEA/H_2O, 0 °C, 16 H, 62% (**15a**), 55% (**15b**); (b) Raney Ni/H_2NNH_2/MeOH, △, 1 h, 93% (**16a**), 91% (**16b**); (c) AllocCl/pyridine/CH_2Cl_2, 0 °C, 16 h, 84% (**17a**), 92% (**17b**); (d) $(COCl)_2$/DMSO/TEA/CH_2Cl_2, −60 °C, 59% (**18a**), 75% (**18b**); (e) Ph_3PCH_3Br/KO^{t}Bu/THF, 0 °C, 2.5 h, 51% (**19a**), 35% (**19b**); (f) HF−pyridine complex, THF, 0 °C, 16 h, 99% (**20a**) or TBAF/THF, 0 °C, 60 min, 96% (**20b**); (g) $(COCl)_2$/DMSO/TEA/CH_2Cl_2, −45 °C, 77% (**21a**), 28% (**21b**); (h) $Pd(PPh_3)_4$/PPh_3/pyrrolidine/CH_2Cl_2, 1.5 h, 77% (**4a**), 75% (**4b**).

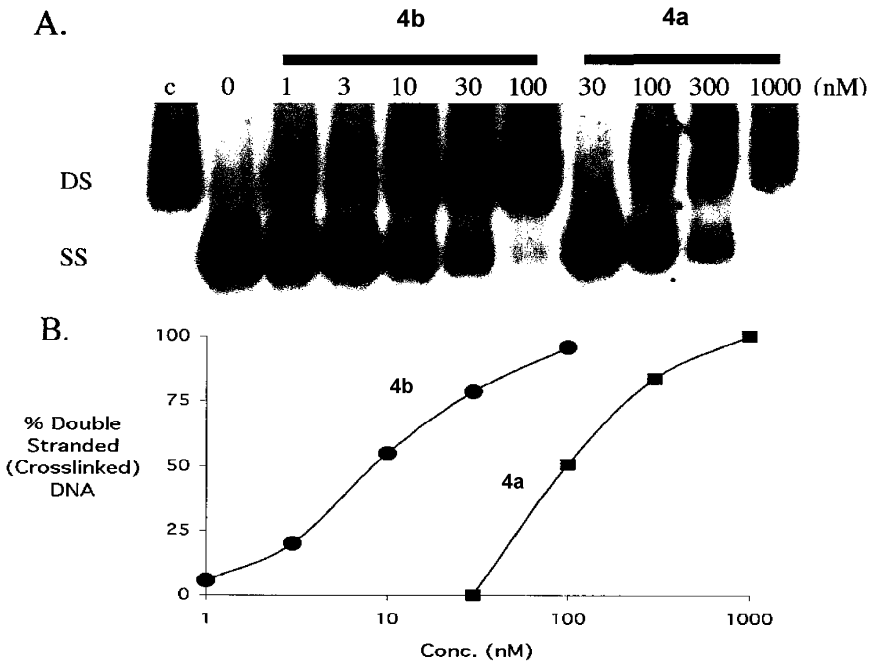

Figure 3. (A) Autoradiograph of a representative agarose gel showing the comparison of interstrand DNA cross-linking by **4b** ($n = 5$) and **4a** ($n = 3$) in linear plasmid puc18 DNA. Drug treatments were for 2 h at the concentrations shown in the figure (c = control). (B) Double-stranded (DS) and single-stranded (SS) DNA bands were quantified by laser densitometry to obtain a dose−response curve.

propane diether-linked compound **21a**. Finally, the bis-Alloc protected carbinolamines **21a**−**b** were treated with Pd(0) in the presence of pyrrolidine to give **4a** and the novel 1,5-pentane-diether linked PBD dimer **4b** in high yields.

Interstrand DNA Cross-Linking In Vitro and In Cells. The extent of DNA cross-linking induced by **4a** and **4b** was determined using the electrophoretic assay method of Hartley and co-workers.[18] Figure 3A shows a typical gel autoradiograph of a comparison of **4a** and **4b**, with the % double-stranded (cross-linked) DNA quantitated in Figure 3B. For the C2/C2′-*exo*-methylene analogues the cross-linking potency is enhanced by approximately 10-fold for **4b** compared to **4a** (i.e., from C_{50} 0.045 to 0.004 μM). This contrasts with the C2-unsubstituted analogues where the cross-linking potency is slightly reduced (i.e., from C_{50} 0.055 to 0.07 μM) when the length of the central $-O(CH_2)_nO-$ linker is increased from $n = 3$ to 5 (i.e., **3a** → **3c)** (see Table 1).

The single-cell gel electrophoresis (Comet) assay was used to measure interstrand cross-linking in the human leukemic cell line K562 following treatment of cells for 1 h with the C2/C2′-*exo*-methylene dimers **4a** and **4b**. A ~3-fold increase in cross-linking of the cellular DNA was detected in the case of **4b** compared to **4a** (Table 1).

In Vitro Cytotoxicity. Dimers **3a**, **3c**, and **4a**,**b** were assessed for their in vitro cytotoxicity in the K562 cell line following a 1 h exposure (Table 1) and also against the NCI 60-cell-line panel (Figure 4). Dimer **4b** is significantly more cytotoxic than the shorter homologue **4a**. In the NCI screen it had a GI_{50} range of 0.001 to 7.94 nM (mean = 0.12 nM) compared to a range of 0.14 to 324 nM (mean = 7.41 nM) for **4a**. Interestingly, the markedly increased activity of the longer compound was not mirrored in the C-ring saturated counterparts **3a** and **3c** (Table 1). Enhancement of cytotoxicity of **4b** compared to **4a** in individual cell lines ranged from a factor of ~30-fold for UACC-257 (melanoma) to >3000-fold for IGROV1 (ovarian).

Table 1. In Vitro Growth Inhibition of K562, DNA Interstrand Cross-Linking, and Induced Thermal Stabilization of DNA by the PBD Dimers **3a**, **3c**, **4a**,**b**, and the Monomer PBD Tomaymycin (**2a**)

		C_{50} (μM)		ΔT_m (°C)[d] after incubation for		
compound	IC_{50} (μM)[a]	naked DNA[b]	in cells[c]	0 h	4 h	18 h
3a ($n = 3$)	0.2[e]	0.055[e]		10.2	13.1	15.1
3c ($n = 5$)	0.5[e]	0.070[e]		3.3	5.9	9.4
4a ($n = 3$)	0.043[f]	0.045[f]	0.03	25.7	31.9	33.6
4b ($n = 5$)	< 0.001	0.004	0.009	24.9	25.5	25.8
2a (tomaymycin)	–	NA[g]	NA	1.0	2.4	2.6

[a] Dose for 50% growth inhibition of human K562 leukemia cells following incubation for 1 h. [b] Dose required to induce 50% cross-linking in naked plasmid pBR322 DNA following incubation with agent for 2 h at 37°C. Results are the mean from at least three independent experiments. [c] Dose required to induce 50% decrease in tail moment of the DNA of K562 cells following a 1 h treatment. [d] Thermal stabilization of duplex-form calf thymus DNA (100 μM in DNAp; $T_m = 67.8 \pm 0.1$ °C) in aqueous buffer (10 mM NaH_2PO_4/Na_2HPO_4, 1 mM Na_2EDTA, pH 7.00), after incubation at 37 °C for times shown. All ΔT_m values are ± 0.1−0.2 °C from replicate experiments with fixed [ligand]/[DNA] = 1:5. Method and analysis as described in ref 26. [e] Data from ref 4. [f] Data from ref 14. [g] NA = not applicable.

Enzyme Inhibition. Several studies have utilized restriction endonuclease inhibition to establish the relative binding affinity of DNA-interactive small-molecule ligands.[19−21] The ability of a PBD compound to inhibit restriction endonucleases was first demonstrated for anthramycin (**2b**).[22] This stimulated the development of a quantitative restriction enzyme digest (RED_{100}) assay in which the inhibition of DNA cleavage by *Bam*H1 was used to probe the DNA binding behavior of PBD monomers.[23] We have now shown that this technique can also be used to study the covalent DNA

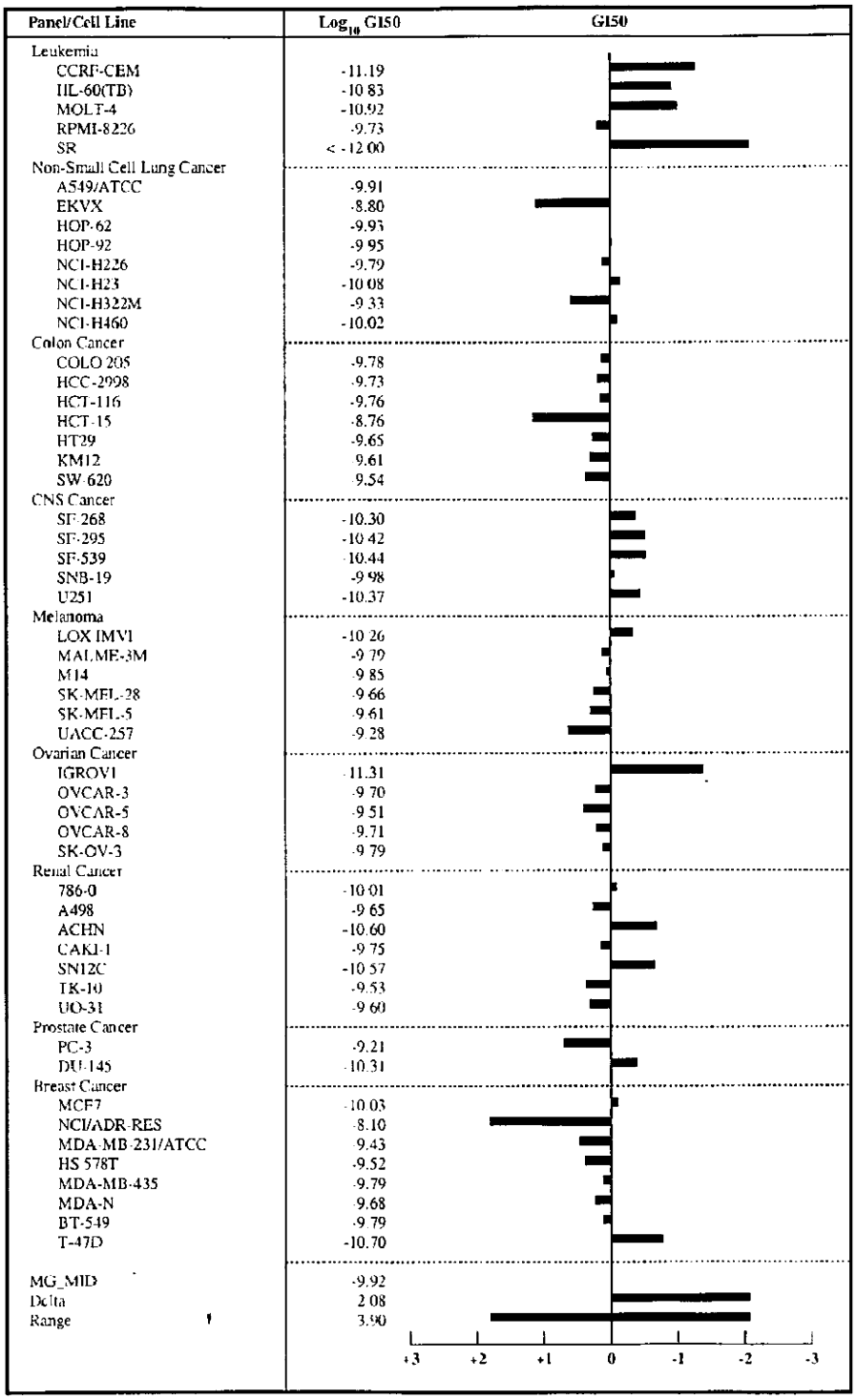

Figure 4. Log_{10} GI_{50} data from the NCI 60 cell line screen for PBD dimer **4b**. The GI_{50} values range from 0.001 to 7.94 nM (mean 0.12 nM).

interaction of PBD dimers and is capable of clearly discriminating between the monomeric and dimeric families.

Figure 5 provides a comparison of the ability of **2b**, **3a**, **4a**, and **4b** to inhibit the cleavage of plasmid pGEM-CAT (see Supporting Information for sequence) by *Bam*HI, the sequence preference of which includes the GATC motif favored by **3a** and **4a**. As anticipated, the total percentage of cut DNA produced from restriction endonuclease digestion decreased as the concentration of the PBD monomer or dimer increased. Each PBD dimer gave an approximately linear dose-dependent response. In terms of dose required to effect 50% inhibition, **4b** is clearly the most effective dimer examined: **4b** (10 μM) > **4a** (17.5 μM) > **3a** (25 μM). The monomer anthramycin (**2b**) was significantly less active in the assay with 25 μM providing only 12% inhibition (50% inhibition could not be achieved in the dose range examined).

There are distinct differences in the inhibitory activity displayed by the PBDs evaluated in this assay. The determined **4b** > **4a** > **3a** ≫ **2b** ranking order for

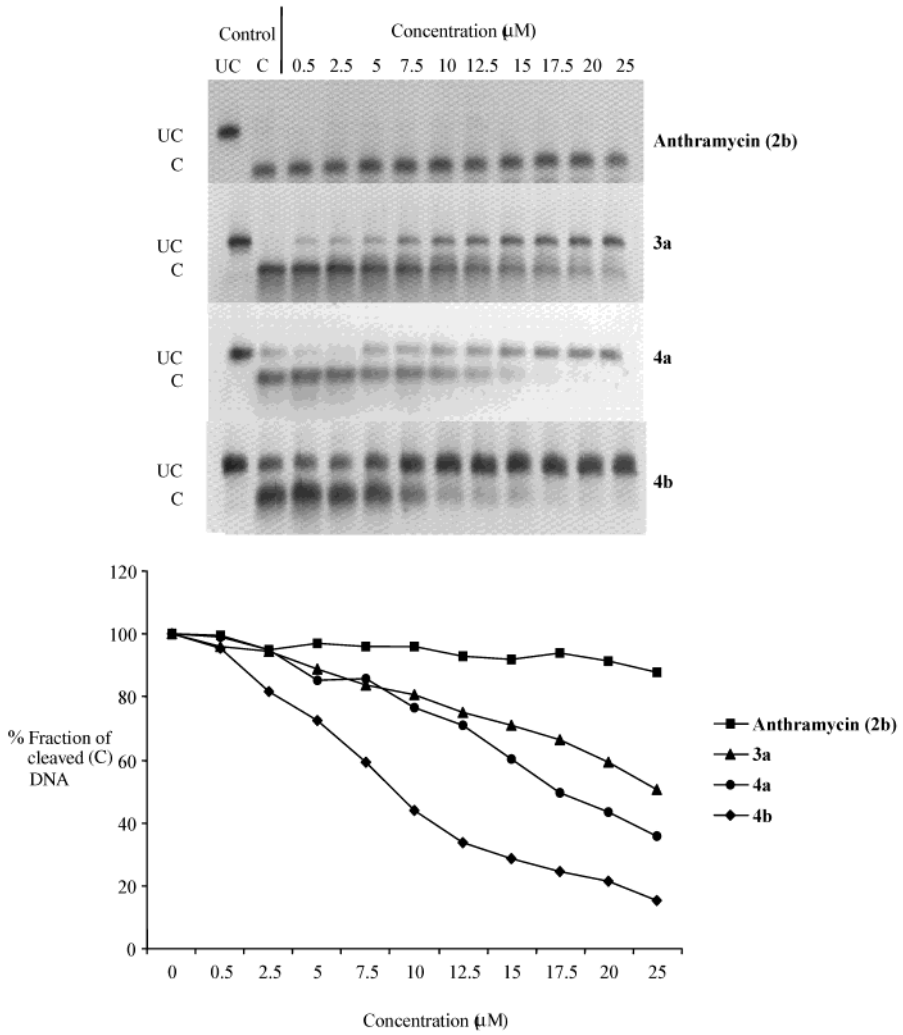

Figure 5. Inhibitory activity of anthramycin (**2b**), **3a**, **4a**, and **4b** on the cleavage of plasmid pGEM-CAT (see Supporting Information) by the restriction endonuclease *Bam*H1. The compounds were incubated at the concentrations shown for 16 h with 500 ng of DNA fragment. The DNA was then digested with *Bam*H1 (10 units) for 1 h under optimal conditions. The cut (C) and uncut (UC) products were separated by electrophoresis on a submarine agarose gel and visualized by ethidium bromide staining under UV illumination (top panel). A permanent record was made, the image was captured and digitized, and the fraction of cut product was calculated and plotted (bottom panel) using ImageQuant software.

inhibition of *Bam*H1 cleavage is in broad agreement with their cytotoxicity and DNA reactivity profiles as profiles measured by thermal denaturation. Furthermore, the time course of binding (data not shown) demonstrated a clear difference between the monomeric (**2b**) and dimeric PBDs (**3a** and **4a**−**b**). For example, the monomer anthramycin (**2b**) requires only 12 h for optimal binding, whereas the dimeric **3a** and **4a**−**b** require 12−24 h for optimal binding, indicating that the monomer binds to DNA more rapidly. This may be due to structural and/or size differences between the two PBD families, and/or to the greater sequence selectivity of binding of the dimers which may lead to a kinetically limiting requirement to find a suitable binding site. As fewer appropriate DNA binding sites are available for dimers compared to monomers, statistical factors may dictate a longer time interval to target and bind to such sites.

Thermal Denaturation Studies. The relative stabilization afforded to double-stranded DNA by the PBD dimers through covalent modification was examined using a thermal denaturation assay, where this UV-based method has been previously used to rank the reactivity of the **3a**−**d** series.[3,4] Natural calf thymus (CT) DNA was used as a host DNA duplex of pseudo-random sequence. Table 1 shows that the T_m for global melting of this duplex is increased upon incubation with the PBD dimers, as expected for a stepwise bifunctional alkylation or cross-linking reaction. This behavior is due to initial non-covalent recognition and binding of the molecule to its favored DNA sites. This is then followed by slower, covalent, reversible "fixation" of the bound ligand. Equilibrium redistribution between mono-alkylated adducts will govern kinetic progress toward the target bis-alkylated (i.e., cross-linked) sites ultimately responsible for biological potency.

Interestingly, the C2-*exo*-unsaturated PBD dimers **4a**−**b** are similarly more effective than the equivalent C-ring saturated compounds **3a** and **3c** in terms of induced ΔT_m shift [i.e., ~8-fold higher for **4b** versus **3c** without DNA−drug incubation ($t = 0$ h)], but exert this effect more rapidly. Thus, while **3a** and **3c** provide 68 and 35% of their maximum (i.e., at $t = 18$ h) effect without prolonged DNA−drug contact (i.e., at $t = 0$), this level increases to 76 and 97% for **4a** and **4b**, respectively. On this basis, **4b** is an unusually rapid and

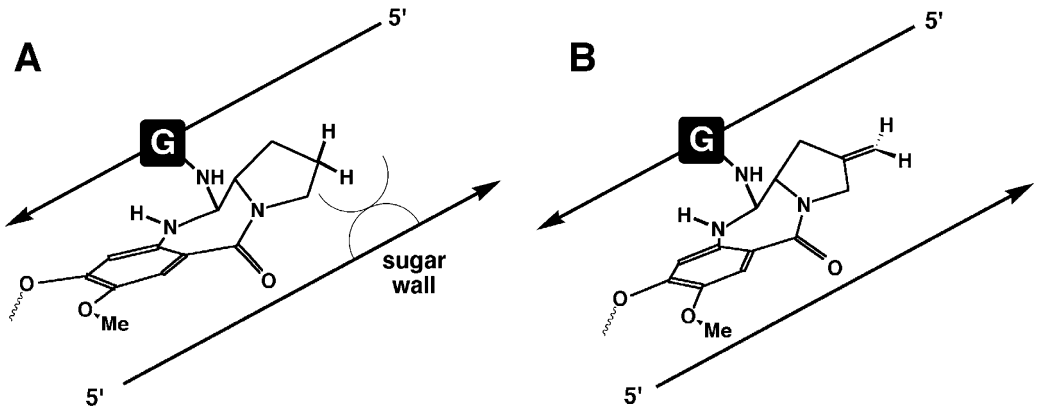

Figure 6. Schematic representation showing the fit of a PBD subunit within the minor groove of a host DNA duplex for (A) **3a**/**3c** and (B) **4a**/**4b** dimers. Localized distortion effects (A) due to steric clash between sugar wall residues and the C2−H atoms of a saturated C-ring are overcome by incorporation of a C2-*exo*-methylene group (B). The groove-spanning hydrogens in (A) are nearly orthogonal in the more isohelical (B) arrangement.

Table 2. Computed Energies for Interstrand Cross-Linking of Target DNA Duplexes[a] by the PBD Dimers **3a**, **3c**, and **4a**,**b**

PBD dimer	*n*	E_{bond} net bonding energy[b]	ΔE_{bind}[c]
3a ($n = 3$)	3	**−70.7**[d,e]	
3c ($n = 5$)	5	**−63.3**	+ 7.4
4a ($n = 3$)	3	**−87.2**[e]	
4b ($n = 5$)	5	**−95.5**	−8.3

[a] Cross-linking of either [d(CGC***G****AT*CGCG)]$_2$ or d(CGC***G****AT*-*T*CGCG)· d(CGC***G****AATC*GCG) duplex by the $n = 3$ and $n = 5$ dimers, respectively (see text). [b] Net bonding enthalpy (kcal mol^{-1}) calculated using $E_{complex} - [E_{DNA} + E_{dimer}]$, following energy minimization. [c] Relative binding enthalpy for the $n = 3 \rightarrow 5$ homologous dimer extension in terms of their energetically favored interstrand cross-linked adducts. [d] A value of −73.1 kcal mol^{-1} was determined for the symmetric **3a**−[d(CIC***G****ATC*ICG)]$_2$ adduct.[8] [e] Values of −88.5 and −104.1 kcal mol^{-1} were reported for the [d(CGCA***G****ATC*TGCG)]$_2$ adducts formed with **3a** and **4a**, respectively.[13]

efficient modifier of duplex DNA. In contrast, the C2-*exo*-unsaturated PBD monomer tomaymycin (**2a**) is of much lower activity and achieves only 38% of its effect in the absence of DNA−drug contact.

Molecular Modeling. Molecular modeling studies for representative d(CGC***G****AT*$_m$*C*GCG)·d(CGC***G****A*$_m$-*TC*GCG) sequences ($m = 1-2$) containing embedded interstrand DNA cross-linking sites indicate that **4b** is a superior ligand compared to **4a**. This is partly due to the longer length of **4b** compared to **4a** and the greater opportunities for contact with the walls of the minor groove. The modeling strategy used and the energetic analysis have previously been detailed for **4a** and the equivalent **3a**−**d** homologous series of saturated C-ring dimers.[7,8,10] The energetically favored cross-link sites for **4a** and **4b** (Table 2) involve 5′-**G**ATC and 5′-**G**ATTC core sequences, respectively, and reflect the different separation of the alkylating PBD subunits in each molecule. Such preferred sequences are identical to those determined for **3a** ($n = 3$) and **3c** ($n = 5$).

Table 2 shows that interstrand DNA−**4b** cross-linking is favorable compared to formation of the shorter adduct with **4a** (−87.2 versus −95.5 kcal mol^{-1} for **4a** and **4b**, respectively; $\Delta E_{bind} = -8.3$ kcal mol^{-1}). In contrast, homologous extension of **3a** to **3c** (i.e., $n = 3 \rightarrow 5$) is markedly disfavored in overall binding energy (−70.7 versus −63.3 kcal mol^{-1}; $\Delta E_{bind} = +7.4$ kcal mol^{-1}) for the equivalent cross-linked adducts.[7] The energetic differences can be explained in terms of superior accommodation of the C2-*exo*-PBD C-rings within the minor groove conduit of the host DNA molecule, such that steric clash between the groove walls and the ring C2-hydrogens of **3a**/**3c** (i.e., the DC-81 subunit) is avoided in the case of **4a**/**4b** (Figure 6).

Importantly, the C2-*exo*-unsaturated C-ring affords a more isohelical fit within the minor groove and hence facilitates improved groove penetration for ligand accommodation. Cross-linking by **4a/4b** is thus favored, compared to the otherwise analogous DNA−**3a/3c** adducts, due to snug shape complementarity ("direct readout") and avoidance of groove conduit perturbation. In the case of the C2-saturated dimers, localized wall distortions induced by the two C-rings are propagated within the spanned site to prevent a full isohelical drug fit of the PBD units and the tethering diether linkage. These disturbances are effectively "tailored out" or ameliorated with the C2-*exo*-methylene dimer compounds. Full details of the energetic analysis, including the induced distortion terms for each reactant, will be reported elsewhere.

Conclusions

The C2/C2′-*exo*-methylene PBD dimer **4b** containing a C8−O(CH$_2$)$_5$O−C8′ diether linkage is the most effective DNA cross-linking agent known to date, clearly surpassing the previously reported shorter homologue **4a** ($n = 3$). The extreme DNA reactivity shown by these dimers presents difficulties in comparing their biophysical characteristics, as the physical limits of the thermal denaturation (T_m) procedure used to evaluate compounds of this type are being approached. The thermal denaturation studies indicate that both **4a** and **4b** are highly efficient modifiers of double-stranded DNA, and that slow kinetic effects of DNA interaction are ameliorated compared to the equivalent **3a** and **3c** ($n = 3$ and 5, respectively) dimer counterparts with saturated pyrrolidine C-rings. It is interesting that the ΔT_m values for **4a** and **4b** are very similar without incubation (25.7 and 24.9 °C, respectively), but differ appreciably after 18 h incubation (33.6 and 25.8 °C, respectively). This agrees with the molecular modeling studies which suggest that **4b** should have a greater DNA cross-linking ability than **4a**.

The finding of nearly equivalent induced ΔT_m values for **4a** and **4b** with natural random-sequence CT-DNA suggests that the standard temperature-scanning assay ($T_m \sim 93$ °C), which has been widely used by many researchers in this area for DNA cross-linking agents, may not be appropriate to predict the DNA binding (or stabilization) behavior of such potent molecules as **4b** at physiological temperatures. Modification of the assay by using different [ligand]/[DNA] molar ratios (e.g., 1:5 → 1:20) to reduce the drug burden and hence lower the overall T_m may be advantageous in this respect. Alternatively, in the future, for compounds of this potency and sequence selectivity, it may be more appropriate to use low-melting oligonucleotide host duplexes that contain base tract sequences appropriate for interstrand DNA cross-linking.

Molecular modeling calculations predict that **4b** > **4a** in terms of their binding energy toward their energetically-favored target sites for interstrand DNA cross-linking. This contrasts to the reported **3a** > **3c** behavior but is supported by the other results reported here. For example, electrophoretic and cell-based DNA cross-linking assays show a significantly greater reactivity for the longer **4b** homologue with demonstrably faster cross-linking. In addition, **4b** is significantly more effective at inhibiting *Bam*H1 cleavage compared to **3a** or **4a**, and has greater in vitro cytotoxicity compared to **4a** in a variety of cell lines.

It is clear that incorporation of C2-*exo* unsaturation into the C-ring of the PBD skeleton is a significant determinant of the kinetics of covalent DNA-binding reactivity. The SAR knowledge gained from this study will be used in the design of further generations of interstrand DNA cross-linking agents targeted to specific sequences in cancer-critical genes.

Experimental Section

Chemistry. General. Progress of reaction was monitored by thin-layer chromatography (TLC) using GF254 silica gel, with fluorescent indicator on glass plates. Visualization of TLC plates was achieved with UV light and I_2 vapour unless otherwise stated. Flash chromatography was performed using silica gel (14 cm column of J.T Baker 30-60 μm). The majority of reaction solvents were purified and used fresh by distillation under nitrogen from the indicated drying agent: CH_2Cl_2 and MeCN (CaH_2), tetrahydrofuran and toluene (sodium benzophenone ketyl), and MeOH (magnesium turnings and catalytic iodine). Extraction and chromatography solvents were purchased from J. T. Baker and used without further purification. All organic chemicals were purchased from Aldrich Chemical Co. Drying agents and inorganic reagents were bought from BDH.

IR spectra were recorded with a Perkin-Elmer FT/IR-Paragon 1000 spectrophotometer. ^{1}H and ^{13}C NMR spectra were obtained on a Jeol GSX 270 MHz (67.8 MHz for ^{13}C NMR spectra), Brüker ARX 250 MHz (62.9 MHz for ^{13}C NMR spectra), or Jeol JNM-LA 400 MHz (100 MHz for ^{13}C NMR spectra) FT-NMR instrument operating at 20 ± 1 °C. Chemical shifts are reported in parts per million (δ ppm) downfield from internal Me_4Si. Spin multiplicities are described as s (singlet), br s (broad singlet), d (doublet), br d (broad doublet), t (triplet), q (quartet), quint (quintet), or m (multiplet). Mass spectra were recorded on a Jeol JMS-DX 303 GC-mass spectrometer or a VG ZAB-SE double-focusing instrument. Electron impact (EI) mass spectra were obtained at 70 eV, chemical ionisation (CI) spectra were obtained using isobutane as reagent gas, and fast atom bombardment (FAB) spectra were recorded using 3-nitrobenzyl alcohol as a matrix with Xe reagent gas. Accurate molecular masses were determined by peak matching using perfluorokerosene (PFK) as an internal standard. Optical rotations were measured at ambient temperature using a Bellingham and Stanley ADP 220 polarimeter.

Bis[2-methoxy-4-(methoxycarbonyl)phenoxy]alkanes 6a,b. Diethyl azodicarboxylate (19.02 mL, 21.04 g, 121 mmol) was added dropwise over 20 min to a stirred solution of methyl vanillate **5** (20 g, 110 mmol) and Ph_3P (43.2 g, 165 mmol) in anhydrous THF (400 mL), and the reaction mixture was allowed to stir at 0 °C for 1 h. The cold reaction mixture was treated dropwise over 30 min with a solution of 1,3-propanediol (3.83 mL, 4.03 g, 53.0 mmol) or 1,5-pentanediol (5.55 mL, 5.52 g, 53.0 mmol) in THF (4 mL). The reaction mixture was allowed to stir overnight at room temperature, and the precipitated product was collected by vacuum filtration. Dilution of the filtrate with MeOH precipitated further product. The combined white precipitate was used in the next step without further purification.

1′,3′-Bis[2-methoxy-4-(methoxycarbonyl)phenoxy]propane (6a). Yield = 12.4 g (58% based on propanediol); ^{1}H NMR (250 MHz, $CDCl_3$) δ 7.64 (dd, 2H, J = 1.8, 8.3 Hz), 7.54 (d, 2H, J = 1.8 Hz), 6.93 (d, 2H, J = 8.5 Hz), 4.30 (t, 4H, J = 6.1 Hz), 3.90 (s, 6H), 3.89 (s, 6H), 2.40 (p, 2H, J = 6.0 Hz).[3]

1′,5′-Bis[2-methoxy-4-(methoxycarbonyl)phenoxy]pentane (6b). Yield = 12.3 g (52% based on pentanediol); ^{1}H NMR (270 MHz, $CDCl_3$) δ 7.65 (dd, 2H, J = 2.0, 8.4 Hz), 7.54 (d, 2H, J = 2.0 Hz), 6.87 (d, 2H, J = 8.4 Hz), 4.10 (t, 4H, J = 6.6 Hz), 3.90 (s, 6H), 3.89 (s, 6H), 2.10-1.90 (m, 4H), 1.85-1.26 (m, 2H).[3]

Bis[2-methoxy-4-(methoxycarbonyl)-5-nitrophenoxy]-alkanes 7a,b. Solid $Cu(NO_3)_2 \cdot 3H_2O$ (7.94 g, 74.3 mmol, **6a** or 16.79 g, 69.5 mmol, **6b**) was added slowly to a stirred solution of the bis-ester (12 g, 29.7 mmol, **6a** or 12 g, 27.8 mmol, **6b**) in acetic anhydride (78 mL, **6a** or 73 mL, **6b**) at 0 °C. The reaction mixture was allowed to stir for 1 h at 0 °C, the ice bath was removed, and the reaction mixture was allowed to warm to room temperature where a mild exotherm, ca. 40 °C, accompanied by the evolution of NO_2 occured at this stage. After the exotherm had subsided stirring at room temperature was continued for 2 h. The reaction mixture was poured into ice water and the aqueous suspension was allowed to stir for 1 h. The resulting yellow precipitate was collected by vacuum filtration and dried in air to afford the desired bis-nitro compound.

1′,3′-Bis[2-methoxy-4-(methoxycarbonyl)-5-nitrophenoxy]propane (7a). Yield = 13.06 g (89%); ^{1}H NMR (250 MHz, $CDCl_3$) δ 7.49 (s, 2H), 7.06 (s, 2H), 4.32 (t, 4H, J = 6.0 Hz), 3.95 (s, 6H), 3.90 (s, 6H), 2.45-2.40 (m, 2H).[3]

1′,5′-Bis[2-methoxy-4-(methoxycarbonyl)-5-nitrophenoxy]pentane (7b). Yield = 14.23 g (98%); ^{1}H NMR (400 MHz, $CDCl_3$ + DMSO-d_6) δ 7.45 (s, 2H), 7.09 (s, 2H), 4.14 (t, 4H, J = 6.3 Hz), 3.97 (s, 6H), 3.90 (s, 6H), 2.20-1.94 (m, 4H), 1.75-1.70 (m, 2H).[3]

Bis(4-carboxy-2-methoxy-5-nitrophenoxy)alkanes 8a,b. These key intermediates were prepared by hydrolysis of **7a,b** according to the method of Thurston.[3]

1′,3′-Bis(4-carboxy-2-methoxy-5-nitrophenoxy) propane (8a). ^{1}H NMR (250 MHz, DMSO-d_6) δ 7.62 (s, 2H), 7.30 (s, 2H), 4.29 (t, 4H, J = 6.0 Hz), 3.85 (s, 6H), 2.30-2.26 (m, 2H).[3]

1′,5′-Bis(4-carboxy-2-methoxy-5-nitrophenoxy)pentane (8b). ^{1}H NMR (400 MHz, $CDCl_3$) δ 7.39 (s, 2H), 7.16 (s, 2H), 4.12 (t, 4H, J = 6.6 Hz), 3.95 (s, 6H), 2.00-1.85 (m, 4H), 1.75-1.67 (m, 2H).[3]

(2*S*,4*R*)-*N*-(Benzyloxycarbonyl)-2-methoxycarbonyl-4-hydroxypyrrolidine (11). A catalytic amount of concentrated H_2SO_4 was added to a solution of the (2*S*,4*R*)-*N*-(benzyloxycarbonyl)-2-carboxy-4-hydroxypyrrolidine (**10**, 80 g, 302 mmol) in anhydrous MeOH (462 mL) at 10 °C. The reaction mixture was refluxed for 3 h, allowed to cool to room temperature, and then treated with Et_3N (66 mL) and stirred for 1 h. Following removal of excess MeOH by rotary evaporation under reduced pressure the residue was dissolved in EtOAc (460 mL), washed with saturated brine, and dried ($MgSO_4$). Filtration and removal of excess solvent in vacuo afforded ester **11** as a

viscous oil. Yield = 84.4 g (100%); $[\alpha]_D^{20} = -59.4°$ ($c = 0.014$, $CHCl_3$); ^1H NMR (270 MHz, $CDCl_3$) (rotamers) δ 7.35−7.26 (m, 5H), 5.13−5.07 (m, 2H), 4.50−4.47 (m, 2H), 3.74/3.54 (s x 2, 3H), 3.69−3.66 (m, 2H), 2.64 (bs, 1H), 2.08−2.04 (m, 1H) 2.35−2.24 (m, 1H); ^{13}C NMR (67.8 MHz, $CDCl_3$) (rotamers) δ 172.7/172.6, 155.0/154.6, 136.4/136.1, 128.1/128.0, 127.8, 127.7, 127.4, 127.3, 127.0, 69.3/68.6, 67.0/66.9, 57.7/57.4, 54.7/54.1, 52.0/51.8, 38.5/37.8; IR (neat) 3435 (br), 3033, 2953, 1750, 1680, 1586, 1542, 1498, 1422, 1357, 1170, 1124, 1084, 1052, 1004, 963, 916, 823, 770, 750, 699, 673 cm^{-1}; MS (FAB) m/z (relative intensity) 302 ([M + Na]$^{+\bullet}$, 21), 280 ([M + H]$^{+\bullet}$, 76), 236 (54), 210 (43), 144 (100), 136 (28); HRMS [M + H]$^{+\bullet}$ calcd for $C_{14}H_{18}NO_5$ m/z 280.1196, found (FAB) m/z 280.1185.

(2*S*,4*R*)-*N*-(Benzyloxycarbonyl)-2-hydroxymethyl-4-hydroxypyrrolidine (12). Solid $LiBH_4$ (9.89 g, 454 mmol) was added portion wise to a solution of the ester **11** (84.4 g, 302 mmol) in anhydrous THF (600 mL) at 0 °C. After the sample was stirred for 30 min at 0 °C, the reaction mixture was allowed to warm to room temperature and then stirred for a further 2 h at room temperature. During this time, a thick suspension formed despite the addition of further THF (150 mL); TLC (EtOAc) at this point revealed the complete disappearance of starting material. The suspension was cooled to 0 °C, diluted with water (389 mL), and treated dropwise with aqueous HCl (2 M, 400 mL) provoking vigorous effervescence. Excess THF was removed by rotary evaporation under reduced pressure, and the aqueous residue was extracted with EtOAc (4 × 250 mL). The combined organic phase was washed with brine (300 mL) and dried over $MgSO_4$. Filtration and solvent removal afforded the product **12** as a transparent, colorless oil. Yield = 73.2 g (96%); $[\alpha]_D^{26} = -42.5°$ ($c = 1$, $CHCl_3$); ^1H NMR (270 MHz, $CDCl_3$) δ 7.34−7.30 (m, 5H), 5.13 (m, 2H), 4.34 (br s, 1H), 4.18−4.04 (m, 1H), 3.80−3.38 (m, 4H), 3.03 (br s, 1H), 2.07−2.00 (m, 2H), 1.73−1.65 (m, 1H); ^{13}C NMR (67.8 MHz, $CDCl_3$) δ 157.2, 136.2, 128.5, 128.2, 127.9, 69.2, 67.4, 66.2, 59.3, 55.6, 37.3; IR (neat) 3390, 3065, 3033, 2953, 1681, 1586, 1538, 1498, 1454, 1192, 1122, 978, 914, 862, 770, 698, 673 cm^{-1}; MS (FAB) m/z (relative intensity) 252 ([M + H]$^{+\bullet}$, 58), 208 (33), 176 (5), 144 (6), 118 (8), 116 (7), 92 (13), 91 (100); HRMS [M + H]$^{+\bullet}$ calcd for $C_{13}H_{18}NO_4$ m/z 252.1226, found (FAB) m/z 252.1236.

(2*S*,4*R*)-*N*-(Benzyloxycarbonyl)-2-*t*-butyldimethylsilyloxymethyl-4-hydroxypyrrolidine (13). *t*-Butyldimethylsilyl chloride (35.9 g, 238 mmol) was added to a solution of the diol **12** (77.8 g, 310 mmol), Et_3N (43.7 mL, 31.7 g, 313 mmol), and DBU (9.17 mL, 9.34 g, 61.3 mmol) in freshly distilled anhydrous CH_2Cl_2 (650 mL). The reaction mixture stirred overnight at room temperature under a N_2 atmosphere. The reaction mixture was washed with saturated aqueous NH_4Cl (300 mL), brine (300 mL), and then dried ($MgSO_4$). Filtration and removal of excess solvent furnished the crude product, which was subjected to flash column chromatography (40:60 v/v EtOAc/40°−60° petroleum ether) to isolate the silyl ether **13**. Yield = 67.9 g (78% based on *t*-butyldimethylsilyl chloride); $[\alpha]_D^{25} = -47.5°$ ($c = 1$, $CHCl_3$); ^1H NMR (270 MHz, $CDCl_3$) (rotamers) δ 7.36−7.29 (m, 5H), 5.21−5.03 (m, 2H), 4.46−4.43 (m, 1H), 4.10−3.99 (m, 1H), 3.70−3.41 (m, 4H), 2.41 (bs, 1H), 2.25−1.95 (m, 2H), 0.86 and 0.84 (s x 2, 9H), 0.01 to −0.07 (m, 6H); ^{13}C NMR (67.8 MHz, $CDCl_3$) (rotamers) δ 155.2/154.9, 136.8/136.5, 128.5, 128.4, 128.1, 127.9, 127.8, 70.2/69.6, 67.0/66.6, 63.9/62.8, 57.8/57.3, 55.7/55.2, 37.2/36.5, 25.8, 18.1, −5.5; IR (neat) 3415 (br), 3066, 3034, 2953, 2930, 2884, 2857, 1703, 1587, 1498, 1424, 1360, 1288, 1255, 1220, 1195, 1118, 1057, 1003, 917, 836, 774, 751, 698, 670 cm^{-1}; MS (FAB) m/z (relative intensity) 388 ([M + Na]$^{+\bullet}$, 20), 365 ([M + H]$^{+\bullet}$, 100), 322 (33), 308 (51), 258 (50); HRMS [M + H]$^{+\bullet}$ calcd for $C_{19}H_{32}NO_4Si$ m/z 366.2103, found (FAB) m/z 366.2101.

(2*S*,4*R*)-2-*t*-Butyldimethylsilyloxymethyl-4-hydroxypyrrolidine (14). A solution of the silyl ether **13** (24.5 g, 67.1 mmol) in absolute anhydrous EtOH (150 mL) over 10% Pd/C (2.45 g) was hydrogenated under pressure (50 psi) on a Parr apparatus for 7.5 h. The reaction mixture was filtered through celite to remove the Pd/C, and the filter pad was washed with hot EtOH. Excess solvent was removed by rotary evaporation under reduced pressure to afford the product **14** as a dark oil. Yield = 15.4 g (99%); $[\alpha]_D^{22} = +35.6°$ ($c = 0.042$, $CHCl_3$); ^1H NMR (270 MHz, $CDCl_3$) δ 4.80 (br s, 2H), 4.42 (br s, 1H), 3.50−3.47 (m, 3H), 3.11 (dd, 1H, J = 4.2, 11.5 Hz), 2.98 (d, 1H, J = 11.7 Hz), 1.93−1.70 (m, 2H), 0.90−0.88 (m, 9H), 0.06 (s, 6H); ^{13}C NMR (67.8 MHz, $CDCl_3$) δ 71.9, 64.3, 58.2, 54.4, 37.2, 25.9, 18.2, −5.40; IR (neat) 3330 (br), 2928, 2857, 1557, 1421, 1331, 1249, 1204, 1191, 1100, 1073, 993, 713 cm^{-1}; MS (CI) m/z (relative intensity) 232 ([M + H]$^{+\bullet}$, 100), 230 (13), 174 (5), 133 (6), 86 (6); HRMS [M + H]$^{+\bullet}$ calcd for $C_{11}H_{26}NO_2Si$ m/z 232.1741, found (FAB) m/z 232.1733.

1,1′-[[(Alkane-1,3-diyl)dioxy]-bis[(2-nitro-5-methoxy-1,4-phenylene)carbonyl]]-bis[(2*S*,4*R*)-2-*t*-butyldimethylsilyloxymethyl-4-hydroxypyrrolidine] 15a,b. A catalytic amount of DMF (5 drops) was added as a stirred suspension of the bis-acid (3.11 g, 6.68 mmol, **8a** or 5.39 g, 10.9 mmol, **8b**) and oxalyl chloride (2.12 g, 1.46 mL, 16.7 mmol, **8a** or 3.47 g, 2.38 mL, 27.3 mmol, **8b**) in anhydrous THF (32 mL, **8a** or 50 mL, **8b**). Initial effervescence was observed followed by the formation of a homogenous solution; however, after the sample was stirred overnight a suspension of the newly formed acid chloride was formed. Excess THF and oxalyl chloride was removed by rotary evaporation under reduced pressure and the acid chloride was resuspended in fresh THF (30 mL, **8a** or 50 mL, **8b**). The acid chloride solution was added dropwise to a solution of the amine **14** (3.87 g, 16.7 mmol, **8a** or 6.3 g, 27.3 mmol, **8b**), Et_3N (2.70 g, 3.72 mL, 26.7 mmol, **8a** or 4.42 g, 6.09 mL, 43.7 mmol, **8b**), and water (0.9 mL, **8a** or 1.47 mL, **8b**) in THF (20 mL, **8a** or 33 mL, **8b**) at 0 °C under a N_2 atmosphere. The reaction mixture was allowed to warm to room temperature and stirring was continued for 3 h. Excess THF was removed by rotary evaporation under reduced pressure, and the resulting residue was partitioned between water and EtOAc (200/200 mL, **8a** or 300/300mL, **8b**). The layers were allowed to separate and the aqueous layer was extracted with EtOAc (3 × 100 mL, **8a** or 3 × 150 mL, **8b**). The combined organic layers were then washed with aqueous NH_4Cl (100 mL, **8a** or 150 mL, **8b**), saturated aqueous $NaHCO_3$ (100 mL, **8a** or 150 mL, **8b**), brine (100 mL, **8a** or 150 mL, **8b**), and dried ($MgSO_4$). Filtration followed by rotary evaporation under reduced pressure afforded the crude product as a dark oil. The crude product was subjected to flash column chromatography (97:3 v/v $CHCl_3$/MeOH) and removal of excess eluent isolated the pure amide **15a,b**.

1,1′-[[(Propane-1,3-diyl)dioxy]-bis[(2-nitro-5-methoxy-1,4-phenylene)carbonyl]]-bis[(2*S*,4*R*)-2-*t*-butyldimethylsilyloxymethyl-4-hydroxypyrrolidine] (15a). Yield = 3.72 g (62%); $[\alpha]_D^{25} = -92.0°$ ($c = 0.26$, $CHCl_3$); ^1H NMR (400 MHz, $CDCl_3$) (rotamers) δ 7.65 (s, 2H), 6.74 (s, 2H), 4.49−4.30 (m, 2H), 4.33 (t, 4H, J = 5.9 Hz), 4.19−4.05 (m, 2H), 3.93 (s, 6H), 3.80−3.71 (m, 2H), 3.35−3.27 (m, 4H), 3.01−2.97 (m, 2H), 2.58 (d, 2H, J = 5.5 Hz), 2.50−2.35 (m, 2H), 2.32−2.27 (m, 2H), 2.10−2.04 (m, 2H), 0.92−0.82 (m, 18H), 0.10 to −0.08 (m, 12H); ^{13}C NMR (100 MHz, $CDCl_3$) δ 166.6, 154.6, 148.2, 137.3, 128.3, 109.5, 108.2, 70.2, 65.2, 62.7, 57.6, 57.4, 56.6, 36.3, 29.0, 25.9, 18.3, −5.29/−5.41; IR (neat) 3392 (br), 2950, 2856, 1623, 1577, 1524, 1459, 1432, 1381, 1338, 1278, 1219, 1184, 1075 1053, 1004, 938, 914, 837, 778, 724, 668, 649 cm^{-1}; MS (FAB) m/z (relative intensity) 893 ([M + H]$^{+\bullet}$, 19), 878 (6), 835 (2), 779 (9), 761 (6), 517 (3), 459 (5), 258 (7), 100 (3), 86 (4), 75 (29), 73 (100), 59 (17), 58 (6).

1,1′-[[(Pentane-1,5-diyl)dioxy]-bis[(2-nitro-5-methoxy-1,4-phenylene)carbonyl]]-bis[(2*S*,4*R*)-2-*t*-butyldimethylsilyloxymethyl-4-hydroxypyrrolidine] (15b). Yield = 5.29 g (55%); $[\alpha]_D^{19} = -103°$ ($c = 1.0$, $CHCl_3$); ^1H NMR (250 MHz, $CDCl_3$) δ 7.65 (s, 2H), 6.76 (s, 2H), 4.52 (bs, 2H), 4.41 (bs, 2H), 4.16-4.11 (m, 6H), 3.92 (s, 6H), 3.76 (d, 2H, J = 9.9 Hz), 3.33 (td, 2H, J = 4.4, 11.3 Hz), 3.08 (d, 2H, J = 11.3 Hz), 2.38-2.27 (m, 2H), 2.14-1.95 (m, 6H), 1.80-1.68 (m, 2H), 0.90 (s, 18H), 0.10 (s, 12H); ^{13}C NMR (67.8 MHz, $CDCl_3$) δ 166.6, 154.5, 148.3, 137.4, 127.9, 109.3, 108.1, 70.2, 69.2, 62.6, 57.5, 57.2, 56.5, 36.3, 28.3, 25.8/25.7, 22.4, 18.1, −5.41/−5.54; IR ($CHCl_3$) 3400 (br), 2952, 2857, 1621, 1578, 1524, 1464, 1435, 1384, 1337, 1277, 1221, 1185, 1117, 1099, 1077, 1052, 1003, 914, 837,

779, 758, 666, 649, 620 cm^{-1}; MS (FAB) *m/z* (relative intensity) 943 ($[M + Na]^{+\bullet}$, 15), 921 ($[M + H]^{+\bullet}$, 100), 863 (34), 789 (11), 690 (9), 346 (49); HRMS $[M + H]^{+\bullet}$ calcd for $C_{43}H_{69}N_4O_{14}Si_2$ *m/z* 921.4349, found (FAB) *m/z* 921.4312.

1,1′-[[(Alkane-1,3-diyl)dioxy]-bis[(2-amino-5-methoxy-1,4-phenylene)carbonyl]]-bis[(2*S*,4*R*)-2-*t*-butyldimethylsilyloxymethyl-4-hydroxypyrrolidine] 16a,b. A solution of hydrazine hydrate (0.74 mL, 0.76 g, 23.7 mmol, **15a** or 1.25 mL, 1.29 g, 40.2 mmol, **15b**) in MeOH (12 mL, **15a** or 20 mL, **15b**) was added dropwise to a solution of the bis-nitro compound (2.12 g, 2.38 mmol, **15a** or 3.6 g, 3.91 mmol, **15b**) in MeOH (40 mL, **15a** or 68 mL, **15b**) gently refluxing over Raney nickel (300 mg, **15a** or 510 mg, **15b** of a thick slurry). After 5 min at reflux TLC (90:10 v/v $CHCl_3$/MeOH) revealed the incomplete consumption of starting material. The reaction mixture was treated with additional Raney nickel (ca. 500 mg) and hydrazine (0.74 mL, **15a** or 1.25 mL, **15b**) in MeOH (12 mL, **15a** or 20 mL, **15b**) resulting in complete consumption of starting material. Excess Raney nickel was added to the reaction mixture to decompose unreacted hydrazine hydrate, and the reaction mixture was then allowed to cool. The reaction mixture was filtered through celite to remove excess Raney nickel, and the filter pad was washed with additional MeOH (Caution! Raney nickel is pyrophoric; do not allow filter pad to dry; use conc. HCl to destroy nickel). The combined filtrate was evaporated by rotary evaporation under reduced pressure, and the residue was redissolved in CH_2Cl_2. The CH_2Cl_2 solution was dried ($MgSO_4$), filtered, and evaporated to afford the product as a foam.

1,1′-[[(Propane-1,3-diyl)dioxy]-bis[(2-amino-5-methoxy-1,4-phenylene)carbonyl]]-bis[(2*S*,4*R*)-2-*t*-butyldimethylsilyloxymethyl-4-hydroxypyrrolidine] (16a). Yield = 1.84 g (93%); $[\alpha]_D^{24} = -94°$ (*c* = 0.25, $CHCl_3$); ^{1}H NMR (270 MHz, $CDCl_3$) δ 6.65 (s, 2H), 6.21 (s, 2H), 4.52 (bs, 2H), 4.35-4.30 (m, 4H), 4.20-4.16 (m, 4H), 3.75 (s, 6H), 3.61-3.35 (m, 12H), 2.30-2.10 (m, 4H), 2.06-1.95 (m, 2H), 0.89-0.84 (m, 18H), 0.04 to −0.01 (m, 12H); ^{13}C NMR (67.8 MHz, $CDCl_3$) δ 170.2, 150.6, 141.1, 140.3, 112.8, 112.6, 102.2, 70.1, 63.8, 62.3, 59.6, 56.8, 56.7, 35.2, 29.8, 25.9, 18.1, −5.41/−5.51; IR (neat) 3359 (br), 2929, 2856, 1621, 1591, 1469, 1433, 1406, 1358, 1346, 1261, 1232, 1175, 1117, 1056, 1006, 866, 835, 776 cm^{-1}; MS (FAB) *m/z* (relative intensity) 833 ($[M + H]^{+\bullet}$, 18), 773 (9), 602 (13), 399 (7), 371 (34), 232 (9), 206 (22), 192 (14), 176 (13), 166 (44), 150 (8), 100 (10), 73 (100).

1,1′-[[(Pentane-1,5-diyl)dioxy]-bis[(2-amino-5-methoxy-1,4-phenylene)carbonyl]]-bis[(2*S*,4*R*)-2-*t*-butyldimethylsilyloxymethyl-4-hydroxypyrrolidine] (16b). Yield = 3.37 g (91%); $[\alpha]_D^{20} = -100°$ (*c* = 0.19, $CHCl_3$); ^{1}H NMR (270 MHz, $CDCl_3$) δ 6.69 (s, 2H), 6.24 (s, 2H), 4.40−3.40 (m, 28H), 2.40−1.60 (m, 10H), 0.88 (s, 18H), 0.03 (s, 12H); ^{13}C NMR (67.8 MHz, $CDCl_3$) δ 170.2, 151.0, 141.4, 140.6, 112.8, 112.3, 102.4, 70.3, 68.4, 62.6, 59.6, 56.8, 35.6, 28.4, 25.9, 22.3, 18.2, −5.39/−5.49; IR (nujol) 3351 (br), 2922, 1713, 1592, 1556, 1515, 1463, 1378, 1260, 1177, 1117, 1058, 1001, 938, 916, 835, 774, 723, 669 cm^{-1}; MS (FAB) *m/z* (relative intensity) 861 ($[M + H]^{+\cdot}$, 20), 803 (7), 630 (12), 399 (100), 346 (32); HRMS $[M + H]^{+\bullet}$ calcd for $C_{43}H_{73}N_4O_{10}Si_2$ *m/z* 861.4865, found (FAB) *m/z* 861.4833.

1,1′-[[(Alkane-1,3-diyl)dioxy]-bis[(2-amino-*N*-allyloxycarbonyl-5-methoxy-1,4-phenylene)carbonyl]]-bis[(2*S*,4*R*)-2-*t*-butyldimethylsilyloxymethyl-4-hydroxypyrrolidine] 17a,b. A solution of allyl chloroformate (0.463 mL, 0.526 g, 4.36 mmol, **16a** or 1.10 mL, 1.25 g, 10.4 mmol, **16b**) in dry CH_2Cl_2 (36 mL, **16a** or 86 mL, **16b**) was added dropwise to a solution of the bis-aniline (1.817 g, 2.18 mmol, **16a** or 4.47 g, 5.28 mmol, **16b**) and pyridine (0.72 g, 0.74 mL, 9.16 mmol, **16a** or 1.72 g, 1.76 mL, 21.7 mmol, **16b**) in CH_2Cl_2 (71 mL, **16a** or 175 mL, **16b**) at 0 °C under a N_2 atmosphere. The reaction mixture was allowed to warm to room temperature and to stir for 3.5 h. At which time TLC (90:10 v/v $CHCl_3$/MeOH) revealed the reaction to be complete. The reaction mixture was diluted with CH_2Cl_2 (20 mL, **16a** or 50 mL, **16b**) and washed with saturated aqueous $CuSO_4$ (2 × 70 mL, **16a** or 2 × 180 mL, **16b**), water (60 mL, **16a** or 160 mL, **16b**), and then brine (60 mL, **16a** or 160 mL, **16b**). The organic phase was dried ($MgSO_4$), filtered, and evaporated under reduced pressure to afford the product as a foam.

1,1′-[[(Propane-1,3-diyl)dioxy]-bis[(2-amino-*N*-allyloxycarbonyl-5-methoxy-1,4-phenylene)carbonyl]]-bis[(2*S*,4*R*)-2-*t*-butyldimethylsilyloxymethyl-4-hydroxypyrrolidine] (17a). Yield = 1.83 g (84%); $[\alpha]_D^{20} = -14°$ (*c* = 0.25, $CHCl_3$); ^{1}H NMR (270 MHz, $CDCl_3$) δ 8.80 (s, 2H), 7.63 (s, 2H), 6.73 (s, 2H), 6.00−5.85 (m, 2H), 5.33 (dd, 2H, *J* = 1.5, 17.2 Hz), 5.22 (dd, 2H, *J* = 1.5, 10.4 Hz), 4.63−4.54 (m, 6H), 4.35−4.27 (m, 2H), 4.26−4.13 (m, 8H), 3.77 (s, 6H), 3.63−3.52 (m, 6H), 2.36−2.03 (m, 6H), 0.89 (s, 18H), 0.00 (s, 12H); ^{13}C NMR (67.8 MHz, $CDCl_3$) δ 169.5, 153.8, 150.3, 144.3, 132.5, 131.7, 118.1, 116.5, 111.6, 106.4, 70.5, 65.8, 65.3, 62.3, 59.9, 57.1, 56.3, 35.5, 29.2, 25.8, 18.1, −5.42/−5.52; IR (neat) 3351 (br), 2931, 2857, 1762, 1722, 1603, 1521, 1463, 1404, 1264, 1222, 1106, 1053, 1015, 936, 872, 837, 775, 629 cm^{-1}.

1,1′-[[(Pentane-1,5-diyl)dioxy]-bis[(2-amino-*N*-allyloxycarbonyl-5-methoxy-1,4-phenylene)carbonyl]]-bis[(2*S*,4*R*)-2-*t*-butyldimethylsilyloxymethyl-4-hydroxypyrrolidine] (17b). Yield = 4.89 g (92%); $[\alpha]_D^{20} = -68.7°$ (*c* = 0.46, $CHCl_3$); ^{1}H NMR (250 MHz, $CDCl_3$) δ 8.89 (br s, 2H), 7.65 (s, 2H), 6.77 (s, 2H), 6.05−5.85 (m, 2H), 5.40−5.19 (m, 4H), 4.70−4.52 (m, 6H), 4.37 (br s, 2H), 4.20−4.00 (m, 4H), 3.77 (s, 6H), 3.70−3.40 (m, 8H), 2.70−2.53 (bs, 2H), 2.27−2.22 (m, 2H), 2.06−1.90 (m, 6H), 1.67−1.64 (m, 2H), 0.88 (s, 18H), 0.03 (s, 12H); ^{13}C NMR (67.8 MHz, $CDCl_3$) δ 169.5, 153.9, 150.5, 144.1, 132.5, 131.9, 118.0, 116.1, 111.6, 105.9, 70.4, 68.6, 65.8, 62.2, 59.8, 57.1, 56.4, 35.5, 28.6, 25.8, 22.4, 18.1, −5.44/−5.54; IR ($CHCl_3$) 3422 (br), 3020, 2955, 1620, 1524, 1465, 1411, 1260, 1215, 1121, 1051, 928, 837, 669, cm^{-1}; MS (FAB) *m/z* (relative intensity) 1051 ($[M + Na]^{+\bullet}$, 38), 1029 ($[M + H]^{+\bullet}$, 77), 971 (49), 946 (16), 798 (62), 740 (30), 714 (21), 509 (100), 469 (59), 372 (71), 318 (33); HRMS $[M + H]^{+\bullet}$ calcd for $C_{51}H_{81}N_4O_{14}Si_2$ *m/z* 1029.5288, found (FAB) *m/z* 1029.5247.

1,1′-[[(Alkane-1,3-diyl)dioxy]-bis[(2-amino-*N*-allyloxycarbonyl-5-methoxy-1,4-phenylene)carbonyl]]-bis[(2*S*)-2-*t*-butyldimethylsilyloxymethyl-4-oxo-pyrrolidine] 18a,b. A solution of dimethyl sulphoxide (1.12 mL, 1.24 g, 15.84 mmol, **17a** or 2.0 mL, 2.2 g, 28.02 mmol, **17b**) in dry CH_2Cl_2 (24 mL, **17a** or 43 mL, **17b**) was added dropwise over 50 min to a stirred solution of oxalyl chloride (3.96 mL of a 2 M solution in CH_2Cl_2, 7.92 mmol, **17a** or 7.0 mL, 14.0 mmol, **17b**) at −60 °C under a N_2 atmosphere. After the sample was stirred at −50 °C for 25 min, a solution of the bis-alcohol (2.64 g, 2.64 mmol, **17a** or 4.80 g, 4.67 mmol, **17b**) in CH_2Cl_2 (40 mL, **17a** or 72 mL, **17b**) was added dropwise over a period of 70 min. The reaction mixture was allowed to stir at −55 °C for 30 min prior to the dropwise addition of a solution of Et_3N (3.63 g, 5.00 mL, 35.9 mmol, **17a** or 6.54 g, 9.0 mL, 63.48 mmol, **17b**) in CH_2Cl_2 (20 mL, **17a** or 37 mL, **17b**). Stirring was continued at −55 °C for 45 min and then allowed to warm to 0 °C. The reaction mixture was diluted with CH_2Cl_2 (20 mL, **17a,b**) washed with cold 1 M HCl (2 × 60 mL, **17a** or 2 × 100 mL, **17b**) and brine (60 mL, **17a** or 100 mL, **17b**), and then dried ($MgSO_4$). Removal of excess solvent afforded the crude product which was purified by flash column chromatography (50:50 v/v EtOAc/40−60° petroleum ether) to yield the pure bis-ketone as a colourless foam (**18a**) or a pale yellow foam (**18b**).

1,1′-[[(Propane-1,3-diyl)dioxy]-bis[(2-amino-*N*-allyloxycarbonyl-5-methoxy-1,4-phenylene)carbonyl]]-bis[(2*S*)-2-*t*-butyldimethylsilyloxymethyl-4-oxo-pyrrolidine] (18a). Yield = 1.56 g (59%); ^{1}H NMR (270 MHz, $CDCl_3$) δ 8.64 (s, 2H), 7.80 (s, 2H), 6.75 (s, 2H), 6.03−5.89 (m, 2H), 5.35 (dd, 2H, *J* = 1.5, 17.2 Hz), 5.25 (dd, 2H, *J* = 1.3, 10.4 Hz), 4.64−4.61 (m, 4H), 4.29 (t, 4H, *J* = 6.1 Hz), 4.13−3.83 (m, 8H), 3.80 (s, 6H), 3.66−3.62 (m, 2H), 2.73 (dd, 2H, *J* = 9.4, 17.9 Hz), 2.51 (d, 2H, *J* = 17.4 Hz), 2.44-2.38 (m, 2H), 0.87 (s, 18H), 0.00 (s, 12H); ^{13}C NMR (67.8 MHz, $CDCl_3$) δ 208.9, 169.1, 153.5, 150.8, 144.3, 132.4, 118.2, 115.1, 110.9, 106.0, 66.1, 65.8, 65.4, 56.5, 55.0, 39.6, 28.9, 25.7, 18.1, −5.68/−5.77; IR (neat) 3308 (br), 2931, 2856, 1765, 1730, 1624, 1602, 1522, 1468, 1407, 1332, 1259, 1204, 1105, 1053, 1010, 937, 870, 837, 808, 778, 674, 657 cm^{-1}.

1,1′-[[(Pentane-1,5-diyl)dioxy]-bis[(2-amino-*N*-allyloxy-

carbonyl-5-methoxy-1,4-phenylene)carbonyl]]-bis[(2*S*)-2-*t*-butyldimethylsilyloxymethyl-4-oxo-pyrrolidine] (18b). Yield = 3.59 g (75%); $[\alpha]_D^{21} = -49.6°$ (c = 0.24, $CHCl_3$); ^{1}H NMR (250 MHz, $CDCl_3$) δ 8.76 (bs, 2H), 7.79 (s, 2H), 6.74 (s, 2H), 6.05−5.88 (m, 2H), 5.40−5.22 (m, 4H), 4.65−4.62 (m, 4H), 4.20−3.60 (m, 20H), 2.74 (dd, 2H, J = 9.3, 17.5 Hz), 2.50 (d, 2H, J = 17.8 Hz), 2.00-1.90 (m, 4H), 1.75−1.65 (m, 2H), 0.86 (s, 18H), 0.05 (s, 12H); ^{13}C NMR (67.8 MHz, $CDCl_3$) δ 209.0, 169.1, 153.5, 151.0, 144.2, 132.4, 118.2, 115.1, 110.8, 105.7, 68.7, 66.1, 65.8, 56.5, 55.0, 39.6, 28.7, 25.7, 22.6, 18.1, −5.70/−5.77; IR (neat) 3436 (br), 2950, 2856, 1763, 1636, 1524, 1463, 1408, 1261, 1216, 1108, 1013, 928, 870, 832, 751 cm^{-1}; MS (FAB) m/z (relative intensity) 1047 ([M + Na]$^{+\bullet}$, 49), 1025 ([M + H]$^{+\bullet}$, 32), 967 (34), 909 (15), 796 (31), 738 (22), 680 (19), 567 (17), 509 (100), 469 (58), 425 (22), 318 (27); HRMS [M + Na]$^{+\bullet}$ calcd for $C_{51}H_{76}N_4O_{14}Si_2Na$ m/z 1047.4794, found (FAB) m/z 1047.4703.

1,1′-[[(Alkane-1,3-diyl)dioxy]-bis[(2-amino-*N*-allyloxycarbonyl-5-methoxy-1,4-phenylene)carbonyl]]-bis[(2*S*)-2-*t*-butyldimethylsilyloxymethyl-4-methylidene-2,3-dihydropyrrole] 19a,b. A solution of potassium-*t*-butoxide in dry THF (0.5 M, 4.00 mL, 2.00 mmol, **18a** or 0.5 M, 25.2 mL, 12.6 mmol, **18b**) was added to a suspension of methyltriphenylphosphonium bromide (0.716 g, 2.00 mmol, **18a** or 4.50 g, 12.6 mmol, **18b**) in dry THF (2.00 mL, **18a** or 15 mL, **18b**). The resulting yellow ylide suspension was allowed to stir at 0 °C for 2 h before the addition of a solution of the bis-ketone (0.50 g, 0.50 mmol, **18a** or 2.48 g, 2.42 mmol, **18b**) in THF (10 mL) at 10 °C. The reaction mixture was allowed to warm to room temperature and stirring was continued for 1 h. The reaction mixture was partitioned between EtOAc (15 mL, **18a** or 100 mL, **18b**) and water (15 mL, **18a** or 100 mL, **18b**); the separated organic layer was washed with brine (20 mL, **18a** or 200 mL, **18b**) and dried ($MgSO_4$). Removal of excess solvent gave a brown oil that was subjected to flash column chromatography (50:50 v/v EtOAc/40−60° petroleum ether) to afford the product as a yellow glass.

1,1′-[[(Propane-1,3-diyl)dioxy]-bis[(2-amino-*N*-allyloxycarbonyl-5-methoxy-1,4-phenylene)carbonyl]]-bis[(2*S*)-2-*t*-butyldimethylsilyloxymethyl-4-methylidene-2,3-dihydropyrrole] (19a). Yield = 250 mg (51%); $[\alpha]_D^{23} = -32°$ (c = 0.265, $CHCl_3$); ^{1}H NMR (270 MHz, $CDCl_3$) δ 8.80 (br s, 2H), 7.84 (s, 2H), 6.81 (s, 2H), 6.00−5.94 (m, 2H), 5.38−5.30 (m, 4H), 4.98 (br s, 4H), 4.63−4.61 (m, 4H), 4.62−3.80 (m, 20H), 2.75−2.69 (m, 4H), 2.40−2.37 (m, 2H), 0.88 (s, 18H), 0.00 (s, 12H); ^{13}C NMR (67.8 MHz, $CDCl_3$) δ 168.7, 153.5, 150 5, 144.0, 132.6, 118.0, 111.4, 107.1, 105.6, 65.7, 65.3, 63.7, 56.6, 36.1, 28.8, 25.8, 18.2, -5.55; IR (neat) 3307 (br), 3082, 2930, 2857, 2360, 1731, 1668, 1599, 1520, 1470, 1404, 1382, 1257, 1201, 1113, 1053, 1024, 941, 837, 776, 667 cm^{-1}; MS (FAB) m/z (relative intensity); 994 ([M]$^{+\bullet}$, 0.2), 185 (42), 181 (37), 179 (13), 163 (10), 149 (25), 147 (14), 110 (9), 105 (11), 93 (100), 91 (41), 87 (11), 75 (43), 73 (54), 61 (22), 57 (46).

1,1′-[[(Pentane-1,5-diyl)dioxy]-bis[(2-amino-*N*-allyloxycarbonyl-5-methoxy-1,4-phenylene)carbonyl]]-bis[(2*S*)-2-*t*-butyldimethylsilyloxymethyl-4-methylidene-2,3-dihydropyrrole] (19b). Yield = 865 mg (35%); $[\alpha]_D^{20} = -78.5°$ (c = 0.24, $CHCl_3$); ^{1}H NMR (400 MHz, $CDCl_3$) δ 8.90 (br s, 2H), 7.83 (s, 2H), 6.82 (s, 2H), 6.05-5.90 (m, 2H), 5.35 (ddd, 2H, J = 1.5, 1.7, 17.2 Hz), 5.24 (dd, 2H, J = 1.3, 10.4 Hz), 4.99 (br s, 2H), 4.91 (br s, 2H), 4.65−4.60 (m, 4H), 4.20−3.60 (m, 20H), 2.70 (br s, 4H), 2.00−1.90 (m, 4H), 1.75-1.63 (m, 2H), 0.88 (s, 18H), 0.03 (s, 12H); ^{13}C NMR (100 MHz, $CDCl_3$) δ 168.8, 153.5, 150 7, 144.9, 144.0, 132.6, 132.0, 118.0, 115.0, 111.5, 107.1, 105.4, 68.7, 65.7, 63.7, 58.1, 56.6, 34.1, 28.8, 25.8, 22.6, 18.2, −5.51/−5.55; IR (neat) 3328, 3083, 3015, 2953, 2931, 2858, 1731, 1670, 1600, 1523, 1464, 1407, 1361, 1333, 1258, 1203, 1178, 1116, 1053, 1006, 939, 837 cm^{-1}.

1,1′-[[(Propane-1,3-diyl)dioxy]-bis[(2-amino-*N*-allyloxycarbonyl-5-methoxy-1,4-phenylene)carbonyl]]-bis[(2*S*)-2-hydroxymethyl-4-methylidene-2,3-dihydropyrrole](20a). An aliquot of hydrogen fluoride/pyridine complex (0.8 mL, 70% HF, 30% pyridine) was added to a solution of the bis-silyl ether **19a** (285 mg, 0.287 mmol) in THF (10 mL) at 0 °C under a N_2 atmosphere. Stirring was continued at 0 °C for 30 min, and the reaction mixture was then allowed to rise to room temperature over 1 h. The reaction mixture was neutralized with sodium bicarbonate and extracted with CH_2Cl_2 (3 × 30 mL). The combined organic phase was washed with brine and dried ($MgSO_4$). Solvent removal of excess solvent under reduced pressure afforded the product **20a** as a yellow gum (218 mg, 99%); ^{1}H NMR (270 MHz, $CDCl_3$) δ 8.60 (br s, 2H), 7.57 (s, 2H), 6.80 (s, 2H), 6.00-5.96 (m, 2H), 5.37-5.30 (m, 4H), 5.00 and 4.93 (2 x br s, 4H), 4.70-4.63 (m, 4H), 4.29-3.73 (m, 20H), 2.80-2.70 (m, 2H), 2.49-2.44 (m, 2H), 2.36-2.28 (m, 2H).[13]

1,1′-[[(Pentane-1,5-diyl)dioxy]-bis[(2-amino-*N*-allyloxycarbonyl-5-methoxy-1,4-phenylene)carbonyl]]-bis[(2*S*)-2-hydroxymethyl-4-methylidene-2,3-dihydropyrrole](20b). A solution of TBAF (3.02 mL of a 1 M solution in THF, 3.02 mmol) was added to the bis-silyl ether (1.23 g, 1.21 mmol) in THF (30 mL) at 0 °C (ice/acetone). The reaction mixture was allowed to warm to room temperature and to stir overnight. The following day, TLC (50:50 v/v EtOAc/40−60° petroleum ether) revealed the complete disappearance of starting material. Saturated aqueous NH_4Cl (150 mL) was added, and the reaction mixture extracted with EtOAc (3 × 60 mL), washed with sat. sodium chloride (150 mL), dried ($MgSO_4$), filtered, and evaporated in vacuo to give a yellow oil. Purification by flash chromatography (97:3 v/v $CHCl_3$/MeOH) provided the pure alcohol **20b** as a white foam. Yield = 916 mg (96%); $[\alpha]_D^{21} = -29.2°$ (c = 0.172, $CHCl_3$); ^{1}H NMR (400 MHz, $CDCl_3$) δ 8.61 (br s, 2H), 7.58 (s, 2H), 6.79 (s, 2H), 6.05-5.90 (m, 2H), 5.35 (ddd, 2H, J = 1.3, 1.5, 17.2 Hz), 5.24 (dd, 2H, J = 1.3, 10.4 Hz), 5.01 (br s, 2H), 4.93 (br s, 2H), 4.65−4.60 (m, 4H), 4.20−3.60 (m, 20H), 2.76 (dd, 2H, , J = 8.4, 15.7 Hz), 2.47 (d, 2H, J = 15.9 Hz), 2.00−1.90 (m, 4H), 1.80−1.63 (m, 2H); ^{13}C NMR (100 MHz, $CDCl_3$) δ 170.3, 153.8, 150.6, 144.5, 143.1, 132.5, 131.0, 118.0, 116.1, 111.1, 108.1, 106.0, 68.6, 65.7, 65.3, 59.8, 56.7, 53.9, 34.2, 28.5, 22.7; IR ($CHCl_3$) 3423 (br), 3019, 1722, 1600, 1524, 1466, 1409, 1333, 1216, 1117, 1052, 667 cm^{-1}; MS (FAB) m/z (relative intensity) 925 ([M + Cs]$^{+\bullet}$, 91), 815 ([M + Na]$^{+\bullet}$, 90), 793 ([M + H]$^{+\bullet}$, 60), 680 (74), 509 (100), 469 (74); HRMS [M + Na]$^{+\bullet}$ calcd for $C_{41}H_{52}N_4O_{12}Na$ m/z 815.3479, found (FAB) m/z 815.3498.

1,1′-[[(Alkane-1,3-diyl)dioxy]-bis(11*S*,11a*S*)-10-(allyloxycarbonyl)-2-alkylidene-11-hydroxy-7-methoxy-1,2,3,10,-11,11a-hexahydro-5*H*-pyrrolo[2,1-*c*][1,4]-benzodiazepin-5-one] 21a,b. A solution of dimethyl sulphoxide (0.61 g, 0.55 mL, 7.75 mmol, **20a** or 0.13 mL, 0.15 g, 0.19 mmol, **20b**) in dry CH_2Cl_2 (10 mL, **20a** or 3 mL, **20b**) was added dropwise over 15 min to a stirred solution of oxalyl chloride (1.84 mL of a 2 M solution in CH_2Cl_2, 3.67 mmol, **20a** or 0.47 mL, 0.93 mmol, **20b**) at −45 °C under a N_2 atmosphere. The reaction mixture was allowed to stir for 35 min at −45 °C followed by addition of a solution of the diol (1.01 g, 1.32 mmol, **20a** or 264 mg, 0.33 mmol, **20b**) in CH_2Cl_2 (10 mL, **20a** or 3 mL, **20b**) at the same temperature over 15 min. After a further 45 min, a solution of Et_3N (1.09 g, 1.50 mL, 10.76 mmol, **20a** or 0.37 mL, 266 mg, 2.63 mmol, **20b**) in CH_2Cl_2 (10 mL, **20a** or 3 mL, **20b**) was added over 15 min. The reaction mixture was allowed to stir at −45 °C for 30 min before being allowed to warm to room temperature over 45 min. The reaction mixture was diluted with CH_2Cl_2 and then washed with 1 M HCl (3 × 50 mL) and brine (50 mL) and dried ($MgSO_4$). Removal of excess solvent gave the crude product, which was purified by flash chromatography (99:1 v/v $CHCl_3$/MeOH) to afford the product as a white glass.

1,1′-[[(Propane-1,3-diyl)dioxy]-bis(11*S*,11a*S*)-10-(allyloxycarbonyl)-11-hydroxy-7-methoxy-2-methylidene-1,2,3,-10,11,11a-hexahydro-5*H*-pyrrolo[2,1-*c*][1,4]-benzodiazepin-5-one] (21a). Yield = 785 mg (78%); ^{1}H NMR (270 MHz, $CDCl_3$) δ 7.23 (s, 2H), 6.75 (s, 2H), 6.00−5.77 (m, 2H), 5.59 (d, 2H, J = 8.8 Hz), 5.27−5.05 (m, 8H), 4.66−4.17 (m, 14H), 3.88 (s, 6H), 3.70−3.65 (m, 2H), 2.95−2.63 (m, 4H), 2.40−2.32 (m, 2H); ^{13}C NMR (67.8 MHz, $CDCl_3$) δ 166.8, 155.9, 150.1, 148.9, 141.8, 132.8, 128.5, 125.6, 118.2, 114.6, 110.7, 109.8, 85.1, 66.8, 65.9, 59.9, 56.1, 50.7, 34.9, 29.7.[13]

1,1′-[[(Pentane-1,5-diyl)dioxy]-bis(11*S*,11a*S*)-10-(ally-

loxycarbonyl)-11-hydroxy-7-methoxy-2-methylidene-1,2,3,-10,11,11a-hexahydro-5*H*-pyrrolo[2,1-*c*][1,4]-benzodiazepin-5-one] (21b). Yield = 69 mg, (26%); $[\alpha]_D^{25} = +151°$ ($c = 0.28$, $CHCl_3$); ^{1}H NMR (400 MHz, $CDCl_3$) δ 7.22 (s, 2H), 6.65 (s, 2H), 5.82−5.70 (m, 2H), 5.58 (d, 2H, $J = 9.7$ Hz), 5.25−5.00 (m, 8H), 5.75−4.35 (m, 4H), 4.30 (d, 2H, $J = 16.1$ Hz), 4.15 (d, 2H, $J = 17.0$ Hz), 4.01 (t, 4H, $J = 6.3$ Hz), 3.90 (s, 6H), 3.64 (t, 2H, $J = 8.7$ Hz), 3.00−2.85 (m, 2H), 2.71 (d, 2H, $J = 16.3$ Hz), 2.00−1.85 (m, 4H), 1.70−1.60 (m, 2H); ^{13}C NMR (62.9 MHz, $CDCl_3$) δ 166.8, 155.9, 150.2, 148.7, 141.7, 131.7, 128.3, 125.1, 118.0, 113.9, 110.5, 109.7, 85.8, 68.9, 66.7, 59.8, 56.1, 50.6, 34.9, 28.4, 22.3; MS (FAB) *m*/*z* (relative intensity) 811 ($[M + Na]^{+\bullet}$, 100), 788 ($[M]^{+\bullet}$, 45), 771 (79), 753 (53), 709 (21), 678 (23), 662 (24), 602 (19), 576 (17); HRMS $[M + H]^{+\bullet}$ calcd for $C_{41}H_{49}N_4O_{12}$ *m*/*z* 789.3347, found (FAB) *m*/*z* 789.3336.

1,1′-[(Propane-1,3-diyl)dioxy]-bis[(11a*S*)-7-methoxy-2-methylidene-1,2,3,11a-tetrahydro-5*H*-pyrrolo-[2,1-*c*][1,4]-benzodiazein-5-one] (4a). This compound was synthesized as described in ref 14.

1,1′-[(Pentane-1,5-diyl)dioxy]-bis[(11a*S*)-7-methoxy-2-methylidene-1,2,3,11a-tetrahydro-5*H*-pyrrolo[2,1-*c*][1,4]-benzodiazepin-5-one] 4b. A catalytic amount of tetrakis(triphenylphosphine)palladium (13 mg, 11.2 μmol) was added to a stirred solution of the bis-alloc-carbinolamine (170 mg, 0.22 mmol), Ph_3P (5.70 mg, 21.6 μmol), and pyrrolidine (31 mg, 37.3 μL, 0.45 mmol) in CH_2Cl_2 (13 mL) under a N_2 atmosphere. The reaction mixture was allowed to warm to room temperature, and the progress of the reaction was monitored by TLC (95:5 v/v $CHCl_3$/MeOH). After 2.5 h, TLC revealed the reaction was complete to give a spot which fluoresced brightly under UV light. The solvent was evaporated under reduced pressure, and the resulting residue was subjected to flash chromatography (98:2 v/v $CHCl_3$/MeOH) to give the bis-imine target molecule **4b** as a pale orange glass which was repeatedly evaporated in vacuo with $CHCl_3$ to provide the imine form. Yield = 85 mg (75%); $[\alpha]_D^{20} = +734°$ ($c = 0.05$, $CHCl_3$); ^{1}H NMR (400 MHz, $CDCl_3$) δ 7.68 (d, 2H, $J =$ 4.4 Hz), 7.49 (s, 2H), 6.80 (s, 2H), 5.19 (br s, 2H), 5.16 (br s, 2H), 4.28 (br s, 4H), 4.15−4.00 (m, 4H), 3.92 (s, 6H), 3.90−3.80 (m, 2H), 3.12 (dd, 2H, $J = 9.0$, 15.9 Hz), 2.95 (d, 2H, $J =$ 15.9 Hz), 2.00−1.85 (m, 4H), 1.72−1.67 (m, 2H); ^{13}C NMR (100 MHz, $CDCl_3$) δ 164.7, 162.4, 150.9, 147.8, 141.6, 140.6, 119.6, 111.4, 110.3, 109.3, 68.7, 56.1, 53.7, 51.3, 35.4, 28.7, 22.5; IR ($CHCl_3$) 3352 (br), 3085, 3013, 2940, 1691, 1602, 1508, 1466, 1434, 1383, 1263, 1216, 1129, 1096, 1066, 1018, 900, 876 cm^{-1}; MS (FAB) *m*/*z* (relative intensity) 601 ($[M + OH]^{+\bullet}$, 46), 585 ($[M + H]^{+\bullet}$, 100), 520 (23), 492 (30), 343 (23), 329 (35), 307 (74); HRMS $[M + H]^{+\bullet}$ calcd for $C_{33}H_{37}N_4O_6$ *m*/*z* 585.2713, found (FAB) *m*/*z* 585.2722.

Determination of In Vitro Cytotoxicity. K562 human chronic myeloid leukemia cells were maintained in RPM1 1640 medium supplemented with 10% fetal calf serum and 2 mM glutamine at 37 °C in a humidified atmosphere containing 5% CO_2 and were incubated with a specified dose of drug for 1 h at 37 °C in the dark. The incubation was terminated by centrifugation (5 min, 300*g*), and the cells were washed once with drug-free medium. Following the appropriate drug treatment, the cells were transferred to 96-well microtiter plates (10^4 cells per well, 8 wells per sample). Plates were then kept in the dark at 37 °C in a humidified atmosphere containing 5% CO_2. The assay is based on the ability of viable cells to reduce a yellow soluble tetrazolium salt, 3-(4,5-dimethylthiazol-2-yl)-2,5-diphenyl-2*H*-tetrazolium bromide (MTT, Aldrich-Sigma), to an insoluble purple formazan precipitate. Following incubation of the plates for 4 days (to allow control cells to increase in number by approximately 10-fold), 20 μL of MTT solution (5 mg/mL in phosphate-buffered saline) was added to each well, and the plates were further incubated for 5 h. The plates were then centrifuged for 5 min at 300*g* and the bulk of the medium pipetted from the cell pellet leaving 10−20 μL per well. DMSO (200 μL) was added to each well and the samples were agitated to ensure complete mixing. The optical density was then read at a wavelength of 550 nm on a Titertek Multiscan ELISA plate reader, and a dose−response curve was constructed. For each curve, an IC_{50} value was read as the dose required to reduce the final optical density to 50% of the control value.

Determination of DNA Interstrand Cross-Linking in Plasmid DNA. The extent of DNA cross-linking induced by each PBD dimer was determined using the electrophoretic assay method of Hartley and co-workers.[18] Closed-circular puc18 DNA was linearized with HindIII, then dephosphorylated, and finally 5′-singly end-labeled using [γ^{32}P]-ATP and polynucleotide kinase. Reactions containing 30−40 ng of DNA were carried out in aqueous TEOA (25 mM triethanolamine, 1 mM EDTA, pH 7.2) buffer at 37 °C in a final volume of 50 μL. Reactions were terminated by addition of an equal volume of stop solution (0.6 M NaOAc, 20 mM EDTA, 100 μg/mL tRNA) followed by precipitation with EtOH. Following centrifugation of the sample, the supernatant was discarded and the pellet was dried by lyophilization. Samples were resuspended in 10 μL of strand separation buffer (30% DMSO, 1 mM EDTA, 0.04% bromophenol blue, and 0.04% xylenecyanol) and denatured by heating to 90 °C for 2.5 min, followed by immersion in an ice/water bath. Control, non-denatured, samples were re-suspended in l0 μL of non-denaturing buffer solution (0.6% sucrose, 0.04% bromophenol blue in aqueous TAE buffer [40 mM Tris, 20 mM acetic acid, 2 mM EDTA, pH 8.1]) and loaded directly onto the gel for comparison.

Electrophoresis was carried out for 14−16 h at 40 V using a 0.8% submerged agarose gel (20 × 25 × 0.5 cm) in TAE buffer. Gels were dried under vacuum for 2 h at 80 °C onto one layer each of Whatman 3MM and DE8I filter papers using a BioRad 583 gel dryer. Autoradiographs were obtained after exposure of Hyperfilm-MP film (Amersham plc, U.K.) to the dried gel for either 4 h with a screen, or overnight without a screen (to obtain a sharper image). Film bands were quantitated using a BioRad GS-670 imaging laser densitometer. Percentage cross-linking was calculated by measuring the total DNA in each lane (summed density for the double-stranded [DS] and single-stranded [SS] bands) relative to the amount of cross-linked DNA (density of DS band alone). A dose−response curve was derived by plotting drug concentration against the determined percentage level of cross-linked DNA.

Determination of DNA Interstrand Cross-Linking in Cells. Full details of the single-cell gel electrophoresis (Comet) assay to measure interstrand cross-link formation in cells are described elsewhere.[24] All procedures were carried out on ice and in subdued lighting. Following drug treatment of cells and immediately before analysis, cells were irradiated (10 Gy) to deliver a fixed number of random DNA strand breaks. After embedding cells in 1% agarose on a pre-coated microscope slide, the cells were lysed for 1 h in lysis buffer (100 mM Na_2-EDTA, 2.5 M NaCl, 10 mM Tris-HCl pH 10.5) containing 1% Triton X-100 added immediately before analysis, and then washed in distilled water at 15 min intervals for 1 h. Slides were then incubated in alkali buffer (50 mM NaOH, 1 mM Na_2EDTA, pH 12.5) for 45 min, followed by electrophoresis in the same buffer for 25 min at 18 V (0.6 V cm^{-1})/250 mA. The slides were finally rinsed in neutralizing buffer (0.5 M Tris-HCl, pH 7.5) followed by saline.

After drying, the slides were stained with propidium iodide (2.5 μg/mL) for 30 min and then rinsed in distilled water. Images were visualized using a NIKON inverted microscope with high-pressure mercury light source, 510−560 nm excitation filter and 590 nm barrier filter at ×20 magnification. Images were captured using an on-line CCD camera and analyzed using Komet Analysis software (Kinetic Imaging, Liverpool, U.K.); 25 cells were analyzed for each duplicate slide. The tail moment for each image was calculated using the software as the product of the percentage DNA in the comet tail and the distance between the means of the head and tail distributions, based on the definition of Olive and co-workers.[25] Interstrand DNA cross-linking was expressed as the percentage decrease in tail moment compared to irradiated controls calculated by the formula:

$$\% \text{ decrease in tail moment} = \left[1 - \left(\frac{\text{TMdi} - \text{TMcu}}{\text{TMci} - \text{TMcu}}\right)\right] \times 100$$

where TMdi = tail moment for the drug-treated irradiated sample, TMcu = tail moment of untreated, unirradiated control, and TMci = tail moment for the untreated irradiated control.

Restriction Endonuclease Inhibition. Stock solutions of each PBD (10 mM) were prepared by dissolving each compound in HPLC-grade methanol (Sigma). These were stored at −20 °C. To produce a plasmid suitable for the assay a 129-bp fragment **(**from the MMTV promoter) was subcloned into the *Sac*1−*Kpn*1 sites within the multiple cloning site of pGEM-CAT, and then transformed into *Escherichia coli* DH-5*λ*. Cells containing the plasmid were cultured, and the DNA was isolated by alkaline lysis. A 512-bp *Pvu*II fragment from this plasmid, containing a single *BamH*1 site, was utilized for all the experiments in this study. Restriction endonuclease *BamH*1 and the relevant buffer were obtained from NEB.

The DNA fragment (500 ng) was incubated with each PBD (see Figure 5 for PBD concentrations) in a final volume of 15 μL for 16 h at 37 °C. Next, 10× *Bam*H1 buffer (2 μL) was added, and the reaction mixture was made up to 20 μL with *Bam*H1 (10 units) and then incubated for 1 h at 37 °C. The reaction mixtures were then loaded onto a 1% agarose (1 × TBE) gel for photography and analysis.[23]

The sequence of plasmid pGEM-CAT is provided in Supporting Information.

Thermal Denaturation Studies. The PBD agents were subjected to DNA thermal melting (denaturation) studies[13,26,27] using calf thymus DNA (CT-DNA, type-I, highly polymerized sodium salt; 42% G+C [Sigma]) at a fixed 100 μM (DNAp = 50 μM bp) concentration, determined using an extinction coefficient of 6600 (M phosphate)$^{-1}$ cm^{-1} at 260 nm.[28] Solutions were prepared in pH 7.00 ± 0.01 aqueous buffer containing 10 mM NaH_2PO_4/Na_2HPO_4 and 1 mM EDTA. Working solutions containing CT-DNA and the test compound (20 μM) were incubated at 37.0 ± 0.1 °C for 0−18 h using an external water bath. Samples were monitored at 260 nm using a Varian-Cary 400 Bio spectrophotometer fitted with a Peltier heating accessory. Heating was applied at a rate of 1 °C/min in the 45−98 °C temperature range, with optical and temperature data sampling at 200 ms intervals. A separate experiment was carried out using buffer alone, and this baseline was subtracted from each DNA melting curve before data treatment. Optical data were imported into the Origin 5 program (MicroCal Inc., Northampton, MA) for analysis. DNA helix → coil transition temperatures (T_m) were determined at the midpoint of the normalized melting profiles using a published analytical procedure.[27] Results are given as the mean ± standard deviation from at least three determinations. Ligand-induced alterations in DNA melting behavior (ΔT_m) are given by $\Delta T_m = T_m$(DNA + ligand) − T_m(DNA), where the T_m value determined for free CT-DNA is 67.82 ± 0.06 °C (averaged from >90 runs). All PBD compounds were dissolved in HPLC-grade MeOH to give working solutions containing ≤0.6% v/v MeOH; T_m results were corrected for the effects of MeOH cosolvent by using a linear correction term. Other [DNAp]/[ligand] molar ratios (i.e., 50:1 and 100:1) were examined in the case of the PBD dimers to ensure that the fixed 5:1 ratio used in this assay did not result in saturation of the host DNA duplex.

Molecular Modeling. The protocol used for simulations of cross-linking between the PDB dimers and host DNA duplexes has previously been detailed for the symmetric **3a**−d(CGC*GATC*GCG)$_2$ complex[8] and adapted for related studies with the homologues **3a**−**3d**.[7] This three-stage MM/MD/MM methodology was selected to enable comparison of binding energies for PBD dimers **4a** and **4b** versus their **3a** and **3c** counterparts, respectively. Briefly, in each case, Verlet molecular dynamics (MD) was performed at 300 K using the Xplor-NIH 2.0.6[29] molecular structure determination package: (i) heating and equilibration to 300 K over the course of 10 ps followed by (ii) 100 ps of production, with coordinate sampling at 1-ps intervals. Averaged coordinate sets were finally relaxed by using Powell molecular mechanics (MM; energy gradient of 0.1 kcal mol^{-1} Å^{-1}) to generate the final cross-linked DNA structures.

Initial coordinates for the host d(CGCG*ATC*GCG)$_2$ and d(CGCG*ATT*CGCG)·d(CGCG*AAT*CGCG) duplexes were generated for an idealized B-DNA conformation. These sequences were selected to enable formation of 1,4- and 1,5-linked adducts where the cross-linked guanine bases located on opposite strands are separated by defined, inert A/T stretches. Starting coordinates for the docked PBD dimers **4a** and **4b** were generated by elaboration of the DSB-120 (**3a**) ligand taken from the reported NMR structural study.[8] Fully extended, antiperiplanar geometries were used for each dimer, with covalent anchoring to the DNA duplex through C11(*S*) linkages in the PBD residues to each of the guanine 2-NH_2 groups disposed on opposite strands of the DNA host. This stereochemistry is favored for covalent attachment of PBD molecules in the minor groove of duplex DNA.[1,7,8,10]

Interactive molecular modeling (SYBYL 6.5; Tripos Inc., St. Louis, MO) and all energy calculations [Xplor-NIH[29] with CHARMM parametrization] were carried out on a Silicon Graphics Octane workstation. Force-field parameters required for the ligands were interpolated from related studies.[8,10,13] Planar restraints were used to maintain planarity for each DNA base, but artificial terms were not necessary to maintain a Watson−Crick duplex geometry. No attempt was made to influence refinements by restraining either internal or terminal base pairs. Solvent and counterion effects were simulated by using a distance-dependent dielectric constant $\epsilon = cr_{ij}$, where $c = 1$ or $c = 4$ for the MD and MM steps, respectively. Covalent binding energy terms were computed for the energy-minimized DNA−dimer adduct structures, relative to the unreacted PBD dimer and DNA duplex, as described previously.[7,8]

Acknowledgment. This work was supported by Cancer Research UK (C180/A1060, S.P.1938/0402, S.P.1938/0201 and S.P.1938/0301 to D.E.T., J.A.H., and T.C.J.) and Yorkshire Cancer Research (Program Grant to T.C.J.). Dr. Robert Schultz at the National Cancer Institute (NCI, USA) is thanked for providing the 60-cell line data for dimer **4b**. Dr C. Robinson (University of Portsmouth) is acknowledged for supplying the pGEM-CAT plasmid. Anthramycin was a gift from Hoffman-La Roche Corporation (New Jersey, USA).

Supporting Information Available: The sequence of plasmid pGEM-CAT. This material is available free of charge via the Internet at http://pubs.acs.org.

References

(1) Thurston, D. E. Advances in the Study of Pyrrolo[2,1-*c*][1,4]-benzodiazepine (PBD) Antitumour Antibiotics. *Molecular Aspects of Anticancer Drug−DNA Interactions*; The Macmillan Press Ltd.: London, UK, London, 1993; pp 54−88.

(2) Bose, D. S.; Thompson, A. S.; Ching, J. S.; Hartley, J. A.; Berardini, M. D.; et al. Rational Design of a Highly Efficient Irreversible DNA Interstrand Cross-Linking Agent Based on the Pyrrolobenzodiazepine Ring-System. *J. Am. Chem. Soc.* **1992**, *114*, 4939−4941.

(3) Thurston, D. E.; Bose, D. S.; Thompson, A. S.; Howard, P. W.; Leoni, A.; et al. Synthesis of Sequence-Selective C8-Linked Pyrrolo[2,1-*c*][1,4]benzodiazepine DNA Interstrand Cross-Linking Agents. *J. Org. Chem.* **1996**, *61*, 8141−8147.

(4) Bose, D. S.; Thompson, A. S.; Smellie, M.; Berardini, M. D.; Hartley, J. A.; et al. Effect of Linker Length on DNA-Binding Affinity, Cross-Linking Efficiency and Cytotoxicity of C8−Linked Pyrrolobenzodiazepine Dimers. *Chem. Commun.* **1992**, 1518−1520.

(5) Smellie, M.; Kelland, L. R.; Thurston, D. E.; Souhami, R. L.; Hartley, J. A. Cellular Pharmacology of Novel C8-Linked Anthramycin-Based Sequence-Selective DNA Minor-Groove Cross-Linking Agents. *Br. J. Cancer* **1994**, *70*, 48−53.

(6) Kamal, A.; Ramesh, G.; Laxman, N.; Ramulu, P.; Srinivas, O.; et al. Design, synthesis, and evaluation of new non-cross-linking pyrrolobenzodiazepine dimers with efficient DNA binding ability and potent antitumor activity. *J. Med. Chem.* **2002**, *45*, 4679−4688.

(7) Smellie, M.; Bose, D. S.; Thompson, A. S.; Jenkins, T. C.; Hartley, J. A.; et al. Sequence-Selective Recognition of Duplex DNA Through Covalent Interstrand Cross-Linking: Kinetic and Molecular Modeling Studies With Pyrrolobenzodiazepine Dimers. *Biochemistry* **2003**, *42*, 8232−8239.
(8) Jenkins, T. C.; Hurley, L. H.; Neidle, S.; Thurston, D. E. Structure of a Covalent DNA Minor-Groove Adduct With a Pyrrolobenzodiazepine Dimer − Evidence For Sequence-Specific Interstrand Cross-Linking. *J. Med. Chem.* **1994**, *37*, 4529−4537.
(9) Mountzouris, J. A.; Wang, J. J.; Thurston, D.; Hurley, L. H. Comparison of a DSB-120 DNA Interstrand Cross-Linked Adduct with the Corresponding Bis-Tomaymycin Adduct − an Example of a Successful Template-Directed Approach to Drug Design Based Upon the Monoalkylating Compound Tomaymycin. *J. Med. Chem.* **1994**, *37*, 3132−3140.
(10) Adams, L. J.; Jenkins, T. C.; Banting, L.; Thurston, D. E. Molecular Modelling of a Sequence-Specific DNA-Binding Agent Based on the Pyrrolo[2,1-*c*][1,4]benzodiazepines. *Pharm. Pharmacol. Commun.* **1999**, *5*, 555−560.
(11) Walton, M. I.; Goddard, P.; Kelland, L. R.; Thurston, D. E.; Harrap, K. R. Preclinical Pharmacology and Antitumour Activity of the Novel Sequence-Selective DNA Minor-Groove Cross-Linking Agent DSB-120. *Cancer Chemother. Pharmacol.* **1996**, *38*, 431−438.
(12) Morris, S. J.; Thurston, D. E.; Nevell, T. G. Evaluation of the Electrophilicity of DNA-Binding Pyrrolo[2,1-*c*][1,4]benzodiazepines by HPLC. *J. Antibiot.* **1990**, *43*, 1286−1292.
(13) Gregson, S. J.; Howard, P. W.; Hartley, J. A.; Brooks, N. A.; Adams, L. J.; et al. Design, synthesis, and evaluation of a novel pyrrolobenzodiazepine DNA-interactive agent with highly efficient cross-linking ability and potent cytotoxicity. *J. Med. Chem.* **2001**, *44*, 737−748.
(14) Gregson, S. J.; Howard, P. W.; Jenkins, T. C.; Kelland, L. R.; Thurston, D. E. Synthesis of a novel C2/C2′-Exo unsaturated pyrrolobenzodiazepine cross-linking agent with remarkable DNA binding affinity and cytotoxicity. *Chem. Commun.* **1999**, 797−798.
(15) Hartley, J. A.; Spanswick, V. J.; Brooks, N.; Clingen, P. H.; McHugh, P. J.; et al. SJG-136 (NSC 694501) A Novel Rationally Designed DNA Minor Groove Interstrand Cross-Linking Agent With Potent and Broad Spectrum Antitumour Activity. Part 1: Cellular Pharmacology, In Vitro and Initial In Vivo Antitumor Activity. *Cancer Res.* **2003**, in revision.
(16) Alley, M. C.; Hollingshead, M. G.; Pacula-Cox, C. M.; Waud, W. R.; Hartley, J. A.; et al. SJG-136 (NSC 694501) A Novel Rationally Designed DNA Minor Groove Interstrand Cross-Linking Agent With Potent and Broad Spectrum Antitumour Activity. Part 2: Efficacy Evaluations. *Cancer Res.* **2003**, in revision.
(17) Bridges, R. J.; Stanley, M. S.; Anderson, M. W.; Cotman, C. W.; Chamberlin, A. R. Conformationally Defined Neurotransmitter Analogues − Selective- Inhibition of Glutamate Uptake by One Pyrrolidine-2,4-Dicarboxylate Diastereomer. *J. Med. Chem.* **1991**, *34*, 717−725.
(18) Hartley, J. A.; Berardini, M. D.; Souhami, R. L. An Agarose-Gel Method for the Determination of DNA Interstrand Cross-Linking Applicable to the Measurement of the Rate of Total and 2nd-Arm Cross-Link Reactions. *Anal. Biochem.* **1991**, *193*, 131−134.
(19) Balcarova, Z.; Mrazek, J.; Kleinwachter, V.; Brabec, V. Cleavage by Restriction Enzymes of DNA Modified with the Antitumor Drug *Cis*-Diamminedichloroplatinum(Ii). *Gen. Physiol. Biophys.* **1992**, *11*, 579−588.
(20) Brabec, V.; Balcarova, Z. Restriction-Enzyme Cleavage of DNA Modified by Platinum(Ii) Complexes. *Eur. J. Biochem.* **1993**, *216*, 183−187.
(21) Collier, D. A.; Thuong, N. T.; Helene, C. Sequence-Specific Bifunctional DNA Ligands Based on Triple-Helix-Forming Oligonucleotides Inhibit Restriction Enzyme Cleavage Under Physiological Conditions. *J. Am. Chem. Soc.* **1991**, *113*, 1457−1458.
(22) Sumner, W.; Bennett, G. N. Anthramycin Inhibition of Restriction Endonuclease Cleavage and Its Use As a Reversible Blocking-Agent in Dna Constructions. *Nucleic Acids Res.* **1981**, *9*, 2105−2119.
(23) Puvvada, M. S.; Hartley, J. A.; Jenkins, T. C.; Thurston, D. E. A Quantitative Assay to Measure the Relative DNA-Binding Affinity of Pyrrolo[2,1-*c*][1,4]benzodiazepine (PBD) Antitumor Antibiotics Based on the Inhibition of Restriction-Endonuclease Bam*H1*. *Nucleic Acids Res.* **1993**, *21*, 3671−3675.
(24) Hartley, J. M.; Spanswick, V. J.; Gander, M.; Giacomini, G.; Whelan, J.; et al. Detection of DNA Interstrand Crosslinking in Clinical Samples Using the Single Cell COMET Assay. *Ann. Oncol.* **1998**, *9*, 645.
(25) Olive, P. L.; Banath, J. P.; Durand, R. E. Heterogeneity in Radiation-Induced DNA Damage and Repair in Tumor and Normal-Cells Measured Using the Comet Assay. *Radiat. Res.* **1990**, *122*, 86−94.
(26) McConnaughie, A. W.; Jenkins, T. C. Novel Acridine-Triazenes as Prototype Combilexins − Synthesis, DNA-Binding, and Biological-Activity. *J. Med. Chem.* **1995**, *38*, 3488−3501.
(27) Jones, G. B.; Davey, C. L.; Jenkins, T. C.; Kamal, A.; Kneale, G. G.; et al. The Non-Covalent Interaction of Pyrrolo[2,1-*c*][1,4]-benzodiazepine-5,11-diones with DNA. *Anti-Cancer Drug Des.* **1990**, *5*, 249−264.
(28) Manzini, G.; Barcellona, M. L.; Avitabile, M.; Quadrifoglio, F. Interaction of Diamidino-2-Phenylindole (DAPI) with Natural and Synthetic Nucleic Acids. *Nucleic Acids Res.* **1983**, *11*, 8861−8876.
(29) Schwieters, C. D.; Kuszewski, J. J.; Tjandra, N.; Clore, G. M. The XPLOR−NIH NMR Molecular Structure Determination Package. *J. Magn. Reson.* **2003**, *160*, 65−73.

JM030897L